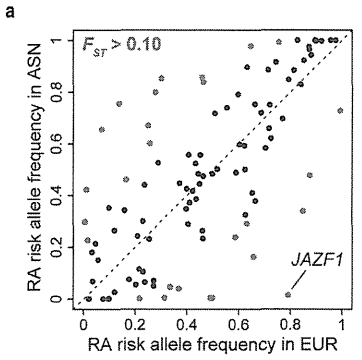

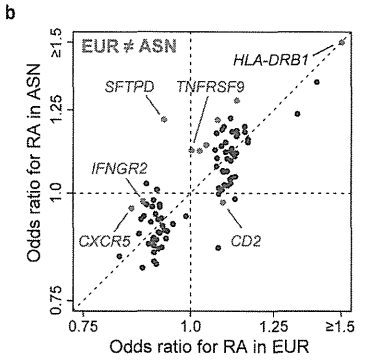

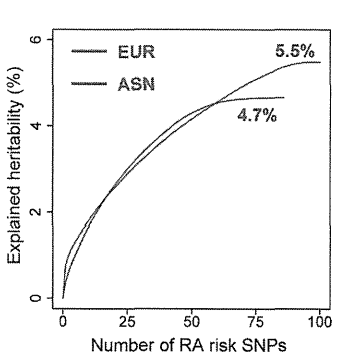

d

Cell types	*P* for H3K4me3 enrichment
T_{reg} primary cells	$\leq 1.0\times10^{-5}$
$CD4^+$ memory primary cells	3.0×10^{-5}
$CD4^+$ naive primary cells	0.0041
$CD8^+$ memory primary cells	0.0065
Smooth muscle, rectal	0.034
Mucosa, colon	0.038
$CD8^+$ naive primary cells	0.12
Mucosa, stomach	0.13
$CD34^+$ primary cells	0.18
$CD34^+$ cultured cells	0.19
Mobilized $CD34^+$ primary cells	0.19
$CD19^+$ primary cells	0.24
$CD3^+$ primary cells	0.30
Mucosa, duodenum	0.40
Muscle satellite cultured cells	0.46
Cingulate gyrus (brain)	0.53
Skeletal muscle	0.77
Mucosa, rectal	0.77
Smooth muscle, colon	0.79
Mesenchymal stem cells (adipose)	0.81
Adipose nuclei	0.84
Smooth muscle, duodenum	0.85
Mid frontal lobe (brain)	0.86
Hippocampus middle (brain)	0.91
Mesenchymal stem cells (bone marrow)	0.91
Pancreatic islets	0.93
Inferior temporal lobe (brain)	0.93
Substantia nigra (brain)	0.93
Adult kidney	0.94
Adult liver	0.95
Mesenchymal stem cells (adipocyte)	0.98
Mesenchymal stem cells (chondrocytes)	0.99
Anterior caudate (brain)	0.99
Smooth muscle, stomach	0.99

e

31 RA risk loci with $P < 10^{-3}$
in EUR and ASN meta-analysis

21.9 SNPs/locus in LD (r^2>0.8) in EUR
37.3 SNPs/locus in LD (r^2>0.8) in ASN
15.0 SNPs/locus in LD (r^2>0.8) in EUR and ASN

⇩

10 RA risk loci significantly enriched with
T_{reg} primary cell H3K4me3 peaks ($P < 0.05$)

10.4 SNPs/locus in LD (r^2>0.8) in EUR and ASN
5.9 SNPs/locus in LD (r^2>0.8) in EUR and ASN
and overlapping with H3K4me3 peaks

f

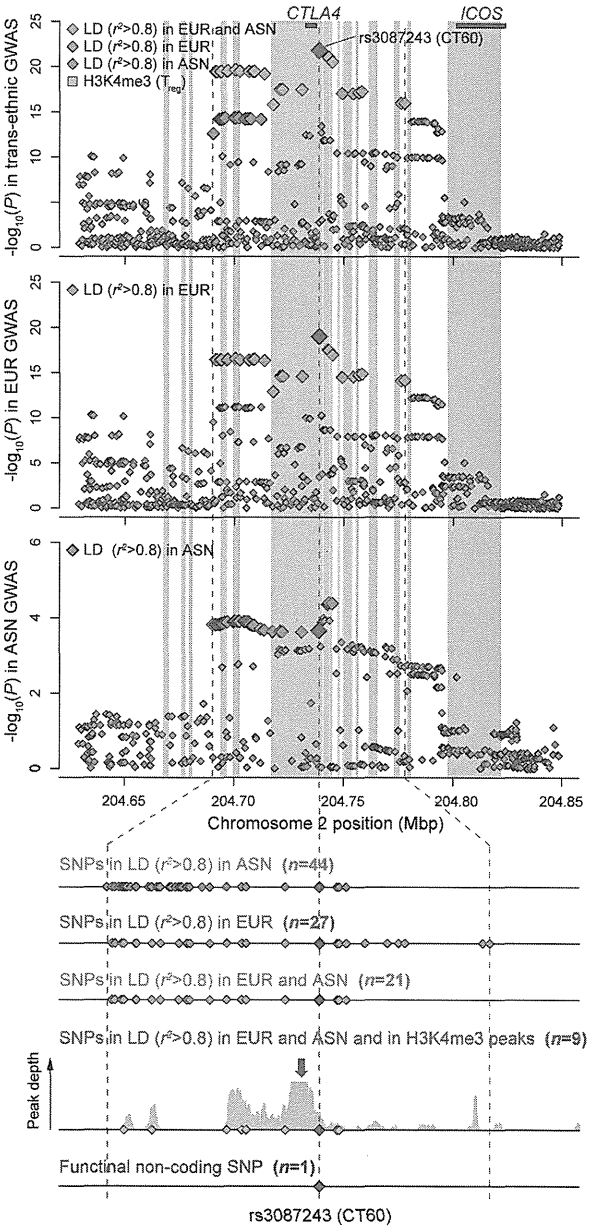

Extended Data Figure 3 | Trans-ethnic and functional annotation of RA risk SNPs. **a**, **b**, Comparisons of RAF and OR values between individuals of European (EUR) and Asian (ASN) ancestry from the stage 1 GWAS meta-analysis. ORs were defined based on minor alleles in Europeans. SNPs with $F_{ST} > 0.10$ or SNPs in which the 95% CI of the OR did not overlap between Europeans and Asians are coloured. OR of the SNP in the *HLA-DRB1* locus ($\geq$1.5) is plotted at the upper limits of the *x*- and *y*-axes. Five loci demonstrated population-specific associations ($P < 5.0 \times 10^{-8}$ in one population but $P > 0.05$ in the other population without overlap of the 95% CI of the OR) are highlighted by red labels (rs227163 at *TNFRSF9*, rs624988 at *CD2*, rs726288 at *SFTPD*, rs10790268 at *CXCR5* and rs73194058 at *IFNGR2*). **c**, Cumulative curve of explained heritability in each population. **d**, Enrichment analysis for overlap of RA risk SNPs with H3K4me3 peaks in cell types. The most significant cell type is T_{reg} primary cells. **e**, Number of SNPs in the process of trans-ethnic and functional fine mapping. For 31 loci in which the risk SNPs yielded $P < 1.0 \times 10^{-3}$ in both populations (stage 1 GWAS), the number of candidate causal variants was reduced by 40–70% when confined by SNPs in linkage disequilibrium with the RA risk SNPs ($r^2 > 0.80$) in both populations (on average, from 21.9 or 37.3 SNPs in linkage disequiliberium in Europeans or Asians, to 15.0 SNPs in linkage disequilibrium in both populations). Further, for 10 loci in which candidate causal variants significantly overlapped with H3K4me3 peaks in T_{reg} cells ($P < 0.05$), the average number of SNPs was further reduced by half again, from 10.4 to 5.9. **f**, Fine mapping in the *CTLA4* locus, where the functional non-coding variant of CT60 (rs3087243)[28] showed the most significant association with RA. The top three panels indicate regional SNP associations of the locus in the stage 1 GWAS meta-analysis for trans-ethnic, European and Asian ancestries, respectively. The bottom panel indicates the change in the number of the candidate causal variants in each process of fine mapping. Trans-ethnic fine mapping of candidate causal variants decreased the number of candidate variants from 44 (linkage disequilibrium in Asians) and 27 (linkage disequilibrium in Europeans) to 21 (linkage disequilibrium in both populations). As these SNPs were significantly enriched in overlap with H3K4me3 peaks in T_{reg} cells compared with the surrounding SNPs ($P = 0.037$), we confined the candidate variants into nine by additionally selecting the SNPs included in H3K4me3 peaks. CT60 was included in these finally selected nine SNPs, and also located at the vicinity of a H3K4me3 peak summit (indicated by a red arrow).

a

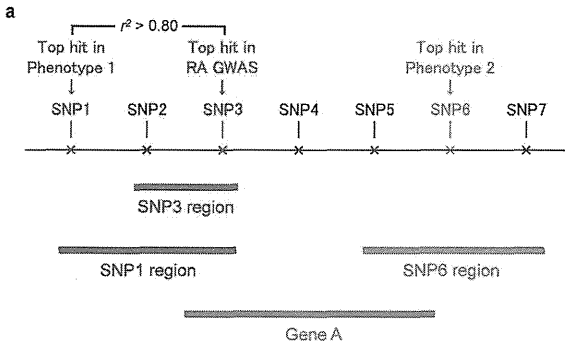

RA and Phenotype 1 : Both region-based and allele-based pleiotropy.

RA and Phenotype 2 : Region-based pleiotropy only.

b

Phenotype in GWAS catalogue	No. loci	Region-based pleiotropy		Allele-based pleiotropy
		No. overlap	P-value	
Type 1 diabetes	42	15	$<1.0\times10^{-7}$	7
Crohn's disease	79	15	$<1.0\times10^{-7}$	4
Systemic lupus erythematosus	22	10	$<1.0\times10^{-7}$	6
Celiac disease	26	10	$<1.0\times10^{-7}$	3
Vitiligo	23	9	$<1.0\times10^{-7}$	3
Primary biliary cirrhosis	22	7	2.4×10^{-6}	3
Alopecia areata	5	4	4.5×10^{-6}	0
Ulcerative colitis	52	9	2.5×10^{-5}	3
Multiple sclerosis	52	9	2.5×10^{-5}	2
Chronic lymphocytic leukemia	9	4	9.1×10^{-5}	0
Kawasaki disease	5	3	2.4×10^{-4}	2
Graves' disease	5	3	2.4×10^{-4}	1
Systemic sclerosis	5	3	2.4×10^{-4}	1
Fibrinogen	8	3	0.0012	1
Asthma	17	4	0.0015	2
Psoriasis	18	4	0.0019	1
Hypothyroidism	4	2	0.0041	2
Basal cell carcinoma	5	2	0.0069	0
Neutrophil count	5	2	0.0069	0
HDL cholesterol	46	5	0.014	1
Eosinophil counts	8	2	0.018	1
C-reactive protein	20	3	0.020	1
Melanoma	11	2	0.034	0
Myasthenia gravis	2	1	0.039	1
Primary sclerosing cholangitis	2	1	0.039	0
Soluble ICAM-1	2	1	0.039	0

c

SNP	Chr.	Position (bp)	A1/A2	Gene	Phenotype	Direction
chr1:2523811	1	2,523,811	G/A	*TNFRSF14-MMEL1*	Multiple sclerosis	Concordant
rs2476601	1	114,377,568	A/G	*PTPN22*	Hypothyroidism	Concordant
					Myasthenia gravis	Concordant
					Crohn's disease	Discordant
					Type 1 diabetes	Concordant
rs2228145	1	154,426,970	A/C	*IL6R*	C-reactive protein	Concordant
					Asthma	Discordant
					sIL-6R	Discordant
					Fibrinogen	Concordant
rs2317230	1	157,674,997	T/G	*FCRL3*	Graves' disease	Concordant
rs34695944	2	61,124,850	C/T	*REL*	Hodgkin lymphoma	Concordant
					Psoriasis	Discordant
rs11889341	2	191,943,742	T/C	*STAT4*	Systemic sclerosis	Concordant
					Systemic lupus erythematosus	Concordant
rs3087243	2	204,738,919	G/A	*CTLA4*	Type 1 diabetes	Concordant
rs11933540	4	26,120,001	C/T	*C4orf52*	Type 1 diabetes	Concordant
rs17264332	6	138,005,515	G/A	*TNFAIP3*	Celiac disease	Concordant
					Ulcerative colitis	Concordant
rs7752903	6	138,227,364	G/T	*TNFAIP3*	Systemic lupus erythematosus	Concordant
chr7:128580042	7	128,580,042	G/A	*IRF5*	Ulcerative colitis	Concordant
					Systemic lupus erythematosus	Concordant
rs2736337	8	11,341,880	C/T	*BLK*	Kawasaki disease	Concordant
					Systemic lupus erythematosus	Concordant
rs1516971	8	129,542,100	T/C	*PVT1*	Ovarian cancer	Concordant
					Crohn's disease	Concordant
rs947474	10	6,390,450	A/G	*PRKCQ*	Type 1 diabetes	Concordant
rs2671692	10	50,097,819	A/G	*WDFY4*	Systemic lupus erythematosus	Concordant
rs726288	10	81,706,973	T/C	*SFTPD*	Serum SP-D levels	Concordant
rs4409785	11	95,311,422	C/T	*CEP57*	Vitiligo	Concordant
rs10790268	11	118,729,391	G/A	*CXCR5*	Primary biliary cirrhosis	Concordant
rs61432431	11	128,322,622	C/T	*ETS1*	Systemic lupus erythematosus	Concordant
rs773125	12	56,394,954	A/G	*CDK2*	Polycystic ovary syndrome	Discordant
					Vitiligo	Discordant
					Type 1 diabetes	Discordant
rs10774624	12	111,833,788	G/A	*SH2B3-PTPN11*	Eosinophil counts	Concordant
					Hypothyroidism	Concordant
					Platelet-related traits	Concordant
					Type 1 diabetes	Concordant
					Blood pressure and hypertension	Concordant
					Vitiligo	Concordant
					Retinal vascular caliber	Concordant
					CKD	Concordant
					Celiac disease	Concordant
rs1950897	14	68,760,141	T/C	*RAD51B*	Primary biliary cirrhosis	Concordant
rs13330176	16	86,019,087	A/T	*IRF8*	Multiple sclerosis	Concordant
chr17:38031857	17	38,031,857	G/T	*IKZF3-CSF3*	Primary biliary cirrhosis	Concordant
					Ulcerative colitis	Concordant
					Crohn's disease	Concordant
					Asthma	Discordant
					Type 1 diabetes	Concordant
rs4239702	20	44,749,251	C/T	*CD40*	Kawasaki disease	Concordant
rs2236668	21	45,650,009	C/T	*ICOSLG-AIRE*	Celiac disease	Concordant
rs11089637	22	21,979,096	C/T	*UBE2L3-YDJC*	Crohn's disease	Concordant
					HDL	Discordant

d

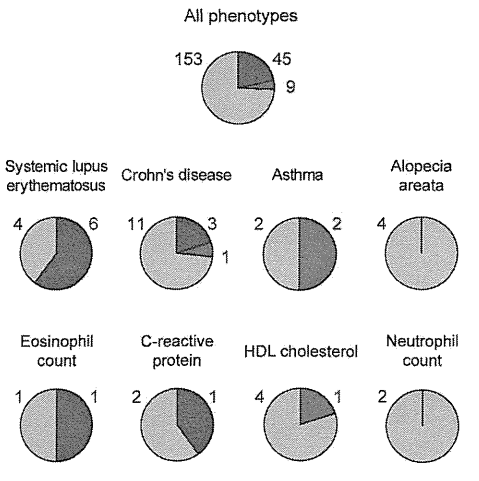

Region- and Allele-based pleiotropy (concordant direction)

Region- and Allele-based pleiotropy (discordant direction)

Region-based pleiotropy only

e

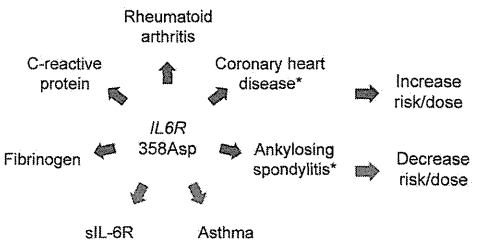

Extended Data Figure 4 | Pleiotropy of RA risk SNPs. **a**, Definition of region-based and allele-based pleiotropy. For each of the RA risk SNPs and SNPs registered in the NHGRI GWAS catalogue (outside of the MHC region), we defined the region on the basis of ±25 kb of the SNP or the neighbouring SNP positions in moderate linkage disequilibrium with it in Europeans or Asians ($r^2 > 0.50$). We defined 'region-based pleiotropy' as two phenotype-associated SNPs sharing part of their genetic regions or any UCSC hg19 reference gene(s) partly overlapping with each of the regions. We defined 'allele-based pleiotropy' as two phenotype-associated SNPs in linkage disequilibrium in Europeans or Asians ($r^2 > 0.80$). **b**, Region-based pleiotropy of the RA risk loci. We found two-thirds of RA risk loci ($n = 66$) demonstrated region-based pleiotropy with other human phenotypes. Phenotypes which showed region-based pleiotropy with RA risk loci are indicated ($P < 0.05$). **c**, Allele-based pleiotropy of the RA risk loci. Allele-based pleiotropy with discordant directional effects to RA risk SNPs are indicated in grey. **d**, Relative proportions of pleiotropic effects (that is, regions and alleles that influence multiple phenotypes) between RA risk loci and 311 phenotypes from the NHGRI GWAS catalogue. Representative examples of disease and biomarker phenotypes are shown. One-quarter of the observed region-based pleiotropic associations (26% = 54/207) were also annotated as having allele-based pleiotropy, although their proportions and directional effects varied among phenotypes. **e**, Allele-based pleiotropy of *IL6R* 358Asp (rs2228145 (A))[5] on multiple disease phenotypes, including increased risk of RA, ankylosing spondylitis and coronary heart disease (asterisks indicate associations obtained from the literature[29,30]) and protection from asthma, as well as levels of biomarkers (increased C-reactive protein (CRP) and fibrinogen but decreased soluble interleukin-6 receptor (sIL6R)).

a

RA risk SNP	r^2	Gene	Missense variants
rs2301888	0.95	*PADI4*	Gly55Ser, Val82Ala, Gly112Ala
rs2476601	1.00	*PTPN22*	Arg620Trp
rs2228145	1.00	*IL6R*	Asp358Ala
rs9826828	0.92	*NCK1*	Ala116Val
	1.00	*NFKBIE*	Val194Ala, Pro175Leu
rs2233424	0.94	*TCTE1*	Arg59His
	0.88	*AARS2*	Val730Met
rs7752903	1.00	*TNFAIP3*	Phe127Cys
rs2671692	0.84	*WDFY4*	Arg1816Gln
rs6479800	0.88	*RTKN2*	Ala288Thr
rs508970	0.90	*CD5*	Ala471Val
rs10774624	0.86	*SH2B3*	Trp262Arg
rs3783782	1.00	*PRKCH*	Val374Ile
rs2582532	1.00	*AHNAK2*	Gly1901Ser
chr17:38031857	0.99	*ZPBP2*	Ser151Ile
	0.99	*GSDMB*	Pro298Ser, Gly291Arg
rs34536443	0.87	*TYK2*	Pro1104Ala
rs2236668	0.94	*ICOSLG*	Trp353Arg
rs5987194	0.96	*IRAK1*	Phe196Ser, Ser453Leu

b

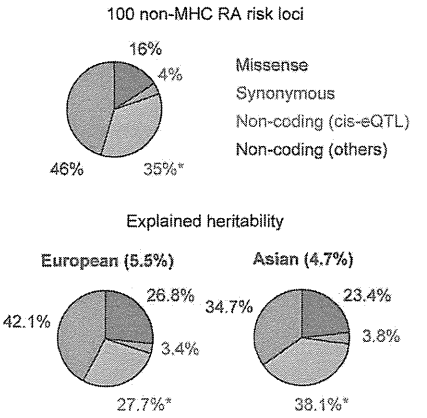

c

	PID classification	No. PID genes	No. overlap with RA genes	Overlap genes	P-value
	All PID genes	194	14	-	1.2×10^{-4}
I	Combined immunodeficiencies	43	3	*PTPRC, RAG1/2, CD40*	0.046
II	Well-defined syndromes	25	2	*ATM, TYK2*	0.12
III	Primary antibody deficiencies	21	2	*CD40, UNG*	0.030
IV	Immune dysregulation	21	4	*CASP8, CASP10, AIRE, IL2RA*	0.0033
V	Phagocyte defects	33	2	*IFNGR2, IRF8*	0.16
VI	Innate immunity	19	0	-	1.0
VII	Autoinflammatory	13	1	*MVK*	0.16
VIII	Complement deficiencies	27	1	*C5*	0.33

d

Cancer type	No. cancer somatic mutation genes	No. overlap with RA genes	Overlap genes	P-value
All cancers	444	23	-	4.7×10^{-5}
Hematological cancers	251	17	-	1.2×10^{-4}
Non-hematological cancers	221	6	-	0.56
Hodgkin lymphoma	10	2	*REL, TNFAIP3*	0.010
B cell non-Hodgkin lymphoma	8	2	*DDX6, FCRL4*	0.015
Non-Hodgkin lymphoma	21	2	*FGFR1OP, HSP90AB1*	0.067
Acute lymphocytic leukemia	29	3	*FCGR2B, AFF3, CDK6*	0.079
Acute myelogenous leukemia	68	2	*ACSL6, PTPN11*	0.47

e

Konckout mouse phenotype category	No. kockout mouse genes with human ortholog	No. overlap with RA genes	P-value
Hematopoietic system phenotype	**2,159**	**86**	**7.0×10^{-6}**
Immune system phenotype	**2,622**	**94**	**1.2×10^{-5}**
Cellular phenotype	**2,961**	**97**	**0.0015**
Liver/biliary system phenotype	982	35	0.0091
Renal/urinary system phenotype	1,028	35	0.011
Endocrine/exocrine gland phenotype	1,453	45	0.020
Respiratory system phenotype	1,097	31	0.028
Tumorigenesis	807	30	0.049
Normal phenotype	1,599	42	0.18
Homeostasis/metabolism phenotype	3,356	88	0.20
Integument phenotype	1,455	35	0.27
Pigmentation phenotype	355	9	0.31
Cardiovascular system phenotype	1,987	42	0.51
Skeleton phenotype	1,435	34	0.57
Other phenotype	258	6	0.57
No phenotypic analysis	1,053	21	0.59
Mortality/aging	3,952	93	0.75
Adipose tissue phenotype	617	12	0.78
Growth/size phenotype	3,061	67	0.79
Digestive/alimentary phenotype	1,128	22	0.80
Reproductive system phenotype	1,730	37	0.81
Limbs/digits/tail phenotype	748	13	0.82
Taste/olfaction phenotype	123	1	0.85
Hearing/vestibular/ear phenotype	557	8	0.88
Embryogenesis phenotype	1,535	30	0.92
Behavior/neurological phenotype	2,465	46	0.94
Nervous system phenotype	2,805	53	0.95
Craniofacial phenotype	951	15	0.96
Muscle phenotype	1,198	21	0.96
Vision/eye phenotype	1,214	21	0.99

f

Database	Molecular pathway	Pathway enrichment (FDR q) Current study	Previous study
BIOCARTA	B Lymphocyte Cell Surface Molecules	**2.0×10^{-4}**	0.26
BIOCARTA	T Cytotoxic Cell Surface Molecules	**3.3×10^{-4}**	**0.032**
BIOCARTA	T Helper Cell Surface Molecules	**4.0×10^{-4}**	**0.030**
BIOCARTA	Th1/Th2 Differentiation	**0.0025**	**0.0063**
Ingenuity	IL-10.Signaling	**0.0026**	0.46
Ingenuity	Interferon.Signaling	**0.0028**	0.13
Ingenuity	GM-CSF.Signaling	**0.0031**	0.43
Ingenuity	T.Cell.Receptor.Signaling	**0.0034**	**0.029**
BIOCARTA	NO2-dependent IL 12 Pathway in NK cells	**0.0044**	0.06
BIOCARTA	IL-22 Soluble Receptor Signaling	**0.0046**	0.39
BIOCARTA	The Co-Stimulatory Signal During T-cell Activation	**0.0046**	0.06
BIOCARTA	Selective expression of chemokine receptors during T-cell polarization	**0.0048**	0.21
Ingenuity	Hepatic.Fibrosis.Hepatic.Stellate.Cell.Activation	**0.0073**	**0.0060**
Ingenuity	p38.MAPK.Signaling	**0.0076**	0.19
Ingenuity	Neuregulin.Signaling	**0.0079**	0.51
Ingenuity	IL-6.Signaling	**0.0082**	0.11
Ingenuity	Glucocorticoid.Receptor.Signaling	**0.0090**	0.18
BIOCARTA	IL-6 signaling	**0.0091**	0.50
BIOCARTA	Influence of Ras and Rho proteins on G1 to S Transition	**0.016**	0.38
BIOCARTA	IL-3 signaling	**0.018**	0.64
BIOCARTA	Adhesion and Diapedesis of Granulocytes	**0.018**	0.15
BIOCARTA	RB Tumor Suppressor/Checkpoint Signaling in response to DNA damage	**0.018**	0.15
Ingenuity	Fc.Epsilon.RI.Signaling	**0.022**	0.19
Ingenuity	JAK.Stat.Signaling	**0.023**	0.48
Ingenuity	IL-2.Signaling	**0.026**	0.17
Ingenuity	PPAR.Signaling	**0.026**	0.24
BIOCARTA	IL-2 Receptor Beta Chain in T cell Activation	**0.027**	0.39
BIOCARTA	Cyclins and Cell Cycle Regulation	**0.028**	0.16
Ingenuity	Leukocyte.Extravasation.Signaling	**0.028**	0.45
BIOCARTA	p53 Signaling Pathway	**0.028**	0.40
BIOCARTA	Role of ERBB2 in Signal Transduction and Oncology	**0.028**	0.51
Ingenuity	B.Cell.Receptor.Signaling	**0.028**	0.45
BIOCARTA	CD40L Signaling	**0.029**	0.16
BIOCARTA	Cells and Molecules involved in local acute inflammatory response	**0.034**	0.40
BIOCARTA	Antigen Dependent B Cell Activation	**0.036**	0.06
BIOCARTA	Adhesion and Diapedesis of Lymphocytes	**0.043**	0.60
BIOCARTA	MAPKinase Signaling	**0.044**	0.76
BIOCARTA	Phosphorylation of MEK1 by cdk5/p35 down regulates the MAP kinase	**0.044**	0.59
Ingenuity	NFKB.Signaling	**0.045**	0.05
Ingenuity	Aryl.Hydrocarbon.Receptor.Signaling	**0.048**	0.33
Ingenuity	PDGF.Signaling	**0.049**	0.30

Extended Data Figure 5 | Overlap of RA risk SNPs with biological resources. **a**, Missense variants in linkage disequilibrium ($r^2 > 0.80$ in Europeans or Asians) with RA risk SNPs. When multiple missense variants are in linkage disequilibrium with the RA risk SNP, the highest r^2 value is indicated. **b**, Functional annotation of the SNPs in 100 non-MHC RA risk loci, including the relative proportion of heritability explained by SNP annotations. Although 44% of all RA risk SNPs had *cis*-eQTL, 9 of them overlapped with missense or synonymous variants but 35 of them did not overlap as indicated by asterisks. A list of *cis*-eQTL SNPs and genes can be found in Extended Data Table 2. **c**, Overlap of RA risk genes with human PID and defined categories. **d**, Overlap of RA risk genes with cancer somatic mutation genes. In addition to the categories of all cancers, haematological cancers and non-haematological cancers, cancer types that showed overlap with ≥2 of RA risk genes are indicated. **e**, Overlap of RA risk genes with knockout mouse phenotypes. Knockout mouse phenotypes that satisfied significant enrichment with RA risk genes are indicated in bold ($P < 0.05/30 = 0.0017$). **f**, Molecular pathway analysis of RA GWAS results. Molecular pathways that showed significant enrichment in either the current stage 1 trans-ethnic GWAS meta-analysis or the previous GWAS meta-analysis of RA[2] are indicated in bold (FDR $q < 0.05$).

a

Biological RA risk gene prioritization criteria

(1) RA risk missense variant (n = 19)
(2) Cis-eQTL (n = 51)
(3) PubMed text-mining (n = 90)
(4) Protein-protein interaction (n = 63)
(5) Primary immunodeficiency (n = 15)
(6) Hematological cancer (n = 17)
(7) Knockout mouse phenotype (n = 86)
(8) Molecular pathway (n = 35)

b

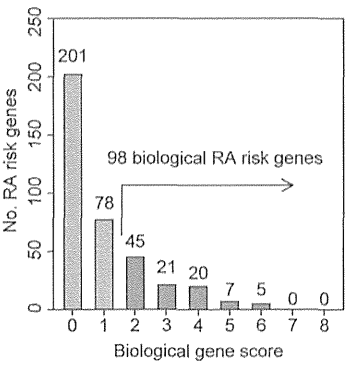

c

Correlation of prioritization criteria of biological genes from RA risk loci (R^2)	RA risk missense variant	Cis-eQTL	PubMed text-mining	Protein-protein interaction	Primary immunodeficiency	Hematological cancer	Knockout mouse phenotype	Molecular pathway
RA risk missense variant	-	0.01	0.03	0.02	0.00	0.00	0.02	0.01
Cis-eQTL	0.01	-	0.05	0.01	0.01	0.00	0.02	0.01
PubMed text-mining	0.03	0.05	-	0.10	0.06	0.03	0.26	0.14
Protein-protein interaction	0.02	0.01	0.10	-	0.04	0.01	0.07	0.06
Primary immunodeficiency	0.00	0.01	0.06	0.04	-	0.00	0.08	0.07
Hematological cancer	0.00	0.00	0.03	0.01	0.00	-	0.03	0.04
Knockout mouse phenotype	0.02	0.02	0.26	0.07	0.08	0.03	-	0.21
Molecular pathway	0.01	0.01	0.14	0.06	0.07	0.04	0.21	-

d

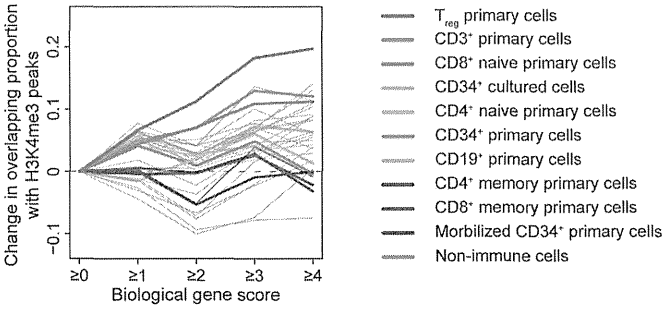

Extended Data Figure 6 | Prioritization of biological candidate genes from RA risk loci. **a**, Prioritization criteria of biological candidate genes from RA risk loci. **b**, Histogram distribution of gene scores. The 98 genes with score ≥2 (orange) were defined as 'biological RA risk genes'. **c**, Correlations of biological candidate gene prioritization criteria. **d**, Change in the overlapping proportions of genes with H3K4me3 peaks by cell type according to score increases. When RA risk SNP of the locus (or SNP in linkage disequilibrium) overlapped with H3K4me3 peaks, genes in the locus were defined as overlapping.

a

RA drug category	Generic name	Target gene
Biologics	Etanercept	*TNF*
	Infliximab	
	Adalimumab	
	Golimumab	
	Certolizumab pegol	
	Abatacept	*CD80, CD86*
	Anakinra	*IL1R1*
	Rituximab	*MS4A1*
	Tocilizumab	*IL6R*
DMARDs	Auranofin	*PRDX5, IKBKB*
	Azathioprine	*HPRT1*
	Cyclophosphamide	-
	Cyclosporine	*CAMLG, PPP3R2*
	Iguratimod (T-614)	*ELANE, PTGS2*
	Leflunomide	*DHODH*
	Methotrexate	*DHFR*
	Sulfasalazine	*ALOX5, PTGS1, PTGS2, PPARG*
	Tacrolimus	*FKBP1A*
	Temsirolimus	*MTOR*
	Tofacitinib (CP-690,550)	*JAK1, JAK2, JAK3*
Steroids	Prednisolone	*NR3C1*
	Methylprednisolone	*NR3C1*
	Desoxycorticosterone Pivalate	*NR3C2*
Others	Hydroxychloroquine	*TLR7, TLR9*

b

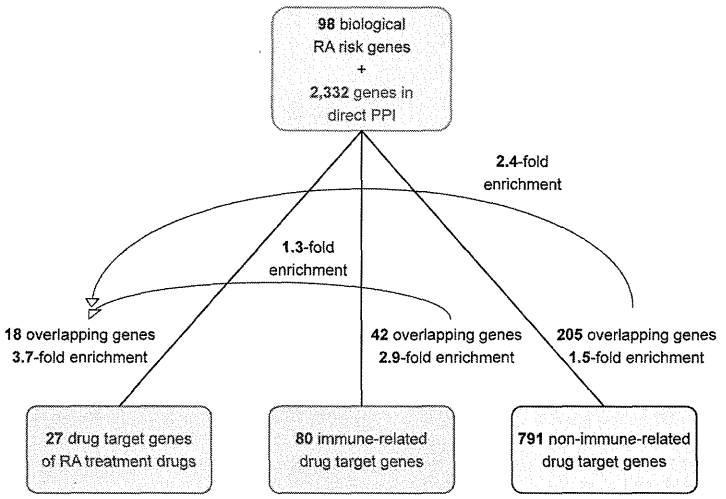

c

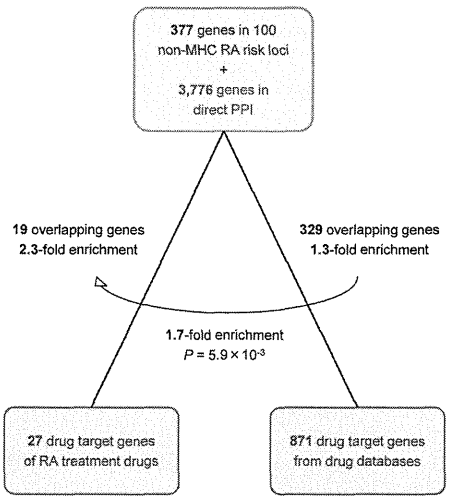

Extended Data Figure 7 | Overlap of all genes in the RA risk loci with drug target genes. **a**, Approved RA drugs and target genes. DMARDs, disease-modifying antirheumatic drugs. **b**, Overlap analysis stratified by immune-related and non-immune-related drug target genes. We made a list of 583 immune-related genes based on Gene Ontology (GO) pathways named 'immune-' or 'immuno-' and found that the majority of drug target genes (791/871 = 91%) were not immune-related. **c**, Overlap of all 377 genes included in 100 RA risk loci (outside of the MHC region) plus 3,776 genes in direct PPI with them and drug target genes. We found overlap of 19 genes from the 27 drug target genes of approved RA drugs (2.3-fold enrichment, $P < 1.0 \times 10^{-5}$). All 871 drug target genes (regardless of disease indication) overlap with 329 genes from the PPI network, which is 1.3-fold more enrichment than expected by chance alone ($P < 1.0 \times 10^{-5}$), but less than 1.7-fold enrichment compared with RA drugs ($P = 0.0059$). We note that this enrichment of drug–gene pairs was less apparent compared with that obtained from the expanded PPI network generated from 98 biological candidate genes (Fig. 3b).

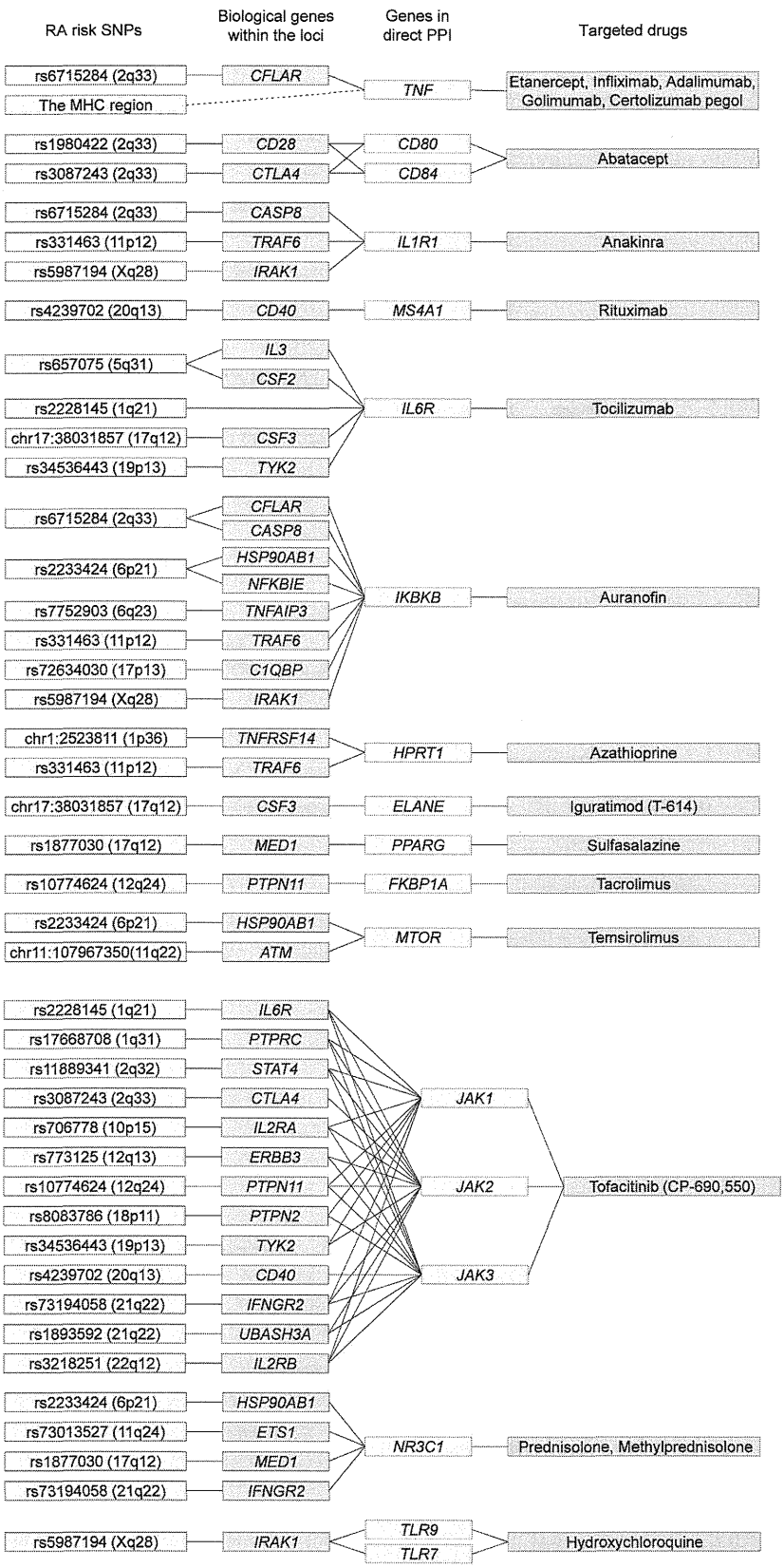

Extended Data Figure 8 | Connection between RA risk genes and approved RA drugs. Full lists of the connections between RA risk SNPs (blue boxes), biological candidate genes from each risk locus (purple boxes), genes from the expanded PPI network (green boxes) and approved RA drugs (orange boxes). Black lines indicate connections. Only *IL6R* is a direct connection between an SNP–biological gene–drug (tocilizumab)[19,20]; all other SNP–drug connections are through the PPI network.

Extended Data Table 1 | Characteristics of the study cohorts

a

Study stage	Cohort	Ethnicity	Geographical origin	No. subjects			RA case sero-positivity
				Cases	Controls	Total	
GWAS meta-analysis (Stage 1)	BRASS	European	North America	483	1,631	2,114	100% CCP+
	CANADA		Canada	589	1,554	2,143	100% CCP+
	EIRA		Sweden	1,097	1,044	2,141	100% CCP+
	NARAC1		North America	863	1,191	2,054	100% CCP+
	NARAC2		North America	896	6,603	7,499	100% CCP+
	WTCCC		United Kingdom	1,520	10,507	12,027	100% CCP+ or RF+
	RACI-UK		United Kingdom	1,645	6,082	7,727	100% CCP+
	RACI-US		North America	997	2,132	3,129	100% CCP+
	RACI-SE-E		Sweden	740	1,117	1,857	100% CCP+
	RACI-SE-U		Sweden	522	962	1,484	100% CCP+
	RACI-NL		Netherland	303	2,001	2,304	100% CCP+
	RACI-ES		Spain	397	399	796	100% CCP+
	RACI-i2b2		North America	882	1,863	2,745	100% CCP+
	ReAct		France	275	804	1,079	70% CCP+ or RF+
	Dutch (AMC, BeSt, LUMC, DREAM)		Netherland	1,172	1,684	2,856	80% CCP+ or RF+
	ACR-REF (BRAGGSS, BRAGGSS2, ERA, KI, TEAR)		North America & Europe	347	264	611	85% CCP+ or RF+
	CORRONA		North America	894	1,838	2,732	61% CCP+ or RF+, 32% unknown
	Vanderbilt		North America	739	2,247	2,986	31% CCP+ or RF+, 56% unknown
	GARNET (BioBank Japan Project; BBJ)	Asian	Japan	2,414	14,245	16,659	79% CCP+, 76% RF+
	GARNET (Kyoto University)		Japan	1,237	2,087	3,324	85% CCP+, 86% RF+
	GARNET (IORRA)		Japan	423	559	982	87% CCP+, 88% RF+
	Korea		Korea	799	751	1,550	100% CCP+
	European	-	-	14,361	43,923	58,284	-
	Asian	-	-	4,873	17,642	22,515	-
	Trans-ethnic	-	-	19,234	61,565	80,799	-
In-silico replication study (Stage 2)	Genentech	European	North America	2,780	4,700	7,480	44% CCP+, 52% unknown 81% RF+, 1.7% unknown
	China	Asian	China	928	835	1,763	48% CCP+
	Total	-	-	3,708	5,535	9,243	-
De-novo replication study (Stage 3)	CANADAII	European	Canada	995	1,101	2,096	100% CCP+
	GARNET	Asian	Japan	5,943	5,557	11,500	81% CCP+, 86% RF+
	Total	-	-	6,938	6,658	13,596	-
Total	European	-	-	18,136	49,724	67,860	-
	Asian	-	-	11,744	24,034	35,778	-
	Trans-ethnic	-	-	29,880	73,758	103,638	-

b

Study stage	Cohort	Genotyping platform	GWAS QC criteria				Imputation method			No.SNPs after QC		Inflation factor		Covariates	X chrom. data
			Sample call rate	SNP call rate	MAF	HWE P-value	Reference panel	MAF	Quality score	Genotyped	Imputed	λ_{GC}	λ_{GC_1000}		
GWAS meta-analysis (Stage 1)	BRASS	Affymetrix Genome-wide Human SNP Array 6.0	>0.95	>0.95	>0.01	$>10^{-6}$	1000 Genomes Phase I (α) Europeans	>0.005	>0.5	649,178	8,201,244	1.015	1.008	Top 5 PCs	Available
	CANADA	Illumina HumanCNV370-Duo BeadChip	>0.95	>0.95	>0.01	$>10^{-6}$	1000 Genomes Phase I (α) Europeans	>0.005	>0.5	295,430	7,933,623	1.002	1.001	Top 5 PCs	Available
	EIRA	HumanHap300 BeadChip	>0.95	>0.95	>0.01	$>10^{-6}$	1000 Genomes Phase I (α) Europeans	>0.005	>0.5	298,193	8,163,538	0.991	0.994	Top 5 PCs	N.A.
	NARAC1	Illumina HumanHap550 BeadChip	>0.95	>0.95	>0.01	$>10^{-6}$	1000 Genomes Phase I (α) Europeans	>0.005	>0.5	479,671	8,254,787	1.017	1.012	Top 5 PCs	N.A.
	NARAC2	HumanHap300 BeadChip	>0.95	>0.95	>0.01	$>10^{-6}$	1000 Genomes Phase I (α) Europeans	>0.005	>0.5	261,974	7,733,592	1.023	1.003	Top 5 PCs	N.A.
	WTCCC	Affymetrix Genome-wide Human SNP Array 5.0	>0.99	>0.99	>0.01	$>10^{-6}$	1000 Genomes Phase I (α) Europeans	>0.005	>0.5	339,790	7,385,370	1.043	1.004	Top 5 PCs	N.A.
	RACI-UK	Illumina Immunochip custom array	>0.99	>0.99	>0.01	$>10^{-6}$	1000 Genomes Phase I (α) Europeans	>0.005	>0.7	126,740	873,840	1.058	1.008	Top 10 PCs	Available
	RACI-US	Illumina Immunochip custom array	>0.99	>0.99	>0.01	$>10^{-6}$	1000 Genomes Phase I (α) Europeans	>0.005	>0.7	120,589	843,395	1.031	1.012	Top 10 PCs	Available
	RACI-SE-E	Illumina Immunochip custom array	>0.99	>0.99	>0.01	$>10^{-6}$	1000 Genomes Phase I (α) Europeans	>0.005	>0.7	124,801	870,585	1.003	1.002	Top 10 PCs	Available
	RACI-SE-U	Illumina Immunochip custom array	>0.99	>0.99	>0.01	$>10^{-6}$	1000 Genomes Phase I (α) Europeans	>0.005	>0.7	123,998	870,797	0.986	0.988	Top 10 PCs	Available
	RACI-NL	Illumina Immunochip custom array	>0.99	>0.99	>0.01	$>10^{-6}$	1000 Genomes Phase I (α) Europeans	>0.005	>0.7	124,480	862,815	1.109	1.051	Top 10 PCs	Available
	RACI-ES	Illumina Immunochip custom array	>0.99	>0.99	>0.01	$>10^{-6}$	1000 Genomes Phase I (α) Europeans	>0.005	>0.7	124,459	859,540	1.081	1.152	Top 10 PCs	Available
	RACI-i2b2	Illumina Immunochip custom array	>0.99	>0.99	>0.01	$>10^{-6}$	1000 Genomes Phase I (α) Europeans	>0.005	>0.7	118,731	829,507	1.003	1.001	Top 10 PCs	Available
	ReAct	Illumina OmniExpress BeadChip Illumina Human 660W-Quad BeadChip	>0.98	>0.99	>0.01	$>10^{-6}$	1000 Genomes Phase I (α) Europeans	>0.005	>0.5	257,299	7,588,538	0.992	0.991	Top 5 PCs	Available
	Dutch	Illumina Human 660W-Quad BeadChip Illumina HumanHap550 BeadChip Illumina HumanCNV370-Duo BeadChip	>0.95	>0.95	>0.01	$>10^{-5}$	1000 Genomes Phase I (α) Europeans	>0.005	>0.5	284,884	7,956,686	1.023	1.011	Top 5 PCs	Available
	ACR-REF	Illumina OmniExpress BeadChip Illumina Human 660W-Quad BeadChip	>0.95	>0.95	>0.01	$>10^{-6}$	1000 Genomes Phase I (α) Europeans	>0.005	>0.5	234,075	7,593,678	1.026	1.070	Top 5 PCs	Available
	CORRONA	Illumina OmniExpress BeadChip	>0.98	>0.99	>0.01	$>10^{-6}$	1000 Genomes Phase I (α) Europeans	>0.005	>0.5	552,896	8,400,238	1.001	1.000	Top 5 PCs	Available
	Vanderbilt	Illumina OmniExpress BeadChip	>0.98	>0.99	>0.01	$>10^{-6}$	1000 Genomes Phase I (α) Europeans	>0.005	>0.5	541,143	8,372,666	0.987	0.995	Top 5 PCs	Available
	BBJ	Illumina HumanHap610-Quad BeadChip	>0.98	>0.99	>0.01	$>10^{-7}$	1000 Genomes Phase I (α) Asians	>0.005	>0.5	477,784	6,874,738	1.038	1.002	-	Available
	Kyoto	Illumina HumaHap610-Quad BeadChip Illumina HumanHap550 BeadChip Illumina HumanCNV370-Duo BeadChip	>0.90	>0.95	>0.05	$>10^{-7}$	1000 Genomes Phase I (α) Asians	>0.005	>0.5	227,348	6,254,431	1.099	1.038	-	N.A.
	IORRA	Affymetrix Genome-wide Human SNP Array 6.0	>0.95	>0.98	>0.05	$>10^{-6}$	1000 Genomes Phase I (α) Asians	>0.005	>0.5	465,832	6,567,923	0.992	0.989	-	Available
	Korea	Illumina Human 660W-Quad BeadChip Illumina HumanHap550 BeadChip	>0.90	>0.90	>0.01	$>10^{-6}$	1000 Genomes Phase I (α) Asians	>0.005	>0.5	418,837	6,424,378	1.007	1.007	-	Available
	European	-	-	-	-	-	-	-	-	-	8,747,962	1.073	1.003	-	-
	Asian	-	-	-	-	-	-	-	-	-	6,619,871	1.041	1.005	-	-
	Trans-ethnic	-	-	-	-	-	-	-	-	-	9,739,303	1.072	1.002	-	-
In-silico replication study (Stage 2)	Genentech	Illumina HumanOmni1-Quad_v1-0_B Illumina Humanhap550K	>0.95	>0.95	>0.10	$>10^{-4}$	1000 Genomes Phase I (α) Europeans	>0.005	>0.5	-	-	-	-	Top 5 PCs	N.A.
	China	Affymetrix Genome-wide Human SNP Array 6.0	>0.95	>0.95	>0.05	$>10^{-3}$	1000 Genomes Phase I (α) Asians	>0.005	>0.5	-	-	-	-	Top 5 PCs	N.A.
De-novo replication study (Stage 3)	CANADAII	iPlex genotyping system	-	-	-	-	-	-	-	-	-	-	-	-	Available
	GARNET	Taqman genotyping system	-	-	-	-	-	-	-	-	-	-	-	-	Available

a, Characteristics of the cohorts and subjects enrolled in the study. **b**, Genotype and imputation methods of the studies. CCP, anti-citrullinated peptide antibody; chrom, chromosome; N.A., not available; PC, principal component; QC, quality control; RF, rheumatoid factor.

Extended Data Table 2 | *cis*-eQTL of RA risk SNPs

a

RA risk SNP	Chr.	Position (bp)	eQTL gene	Cis-eQTL effect of best proxy SNP				Cis-eQTL effect of top eQTL SNP			
				Proxy SNP	Position (bp)	eQTL *P*	r^2	eQTL SNP	Position (bp)	eQTL *P*	r^2
chr1:2523811	1	2,523,811	*PLCH2*	rs10910099	2,533,552	2.2E-18	0.87	rs2494435	2,359,280	2.6E-45	<0.25
			TNFRSF14	rs2843401	2,528,133	1.1E-28	0.87	rs734999	2,513,216	2.1E-90	0.43
rs227163	1	7,961,206	*PARK7*	rs227163	7,961,206	4.6E-10	1.00	rs3766606	8,022,197	1.0E-53	<0.25
rs28411352	1	38,278,579	*MANEAL, YRDC*	rs2306627	38,260,503	3.9E-09	0.84	rs2306426	36,451,618	7.7E-10	<0.25
			INPP5B	rs2306627	38,260,503	7.5E-23	0.84	rs4072980	38,456,106	1.2E-113	<0.25
			SF3A3	rs2306627	38,260,503	3.3E-17	0.84	rs4072980	38,456,106	1.1E-190	<0.25
			FHL3	rs2306627	38,260,503	1.1E-11	0.84	rs4634868	38,465,315	9.8E-198	<0.25
rs2476601	1	114,377,568	*PTPN22*	rs2476601	114,377,568	3.4E-10	1.00	rs7555634	114,367,116	5.3E-43	<0.25
			AQP10	rs6684439	154,395,839	3.3E-06	0.89	rs6688968	154,293,675	3.8E-40	<0.25
rs2228145	1	154,426,970	*IL6R*	rs4129267	154,426,264	3.2E-27	1.00	rs4537545	154,418,879	2.0E-29	0.96
			UBE2Q1	rs4129267	154,426,264	9.7E-08	1.00	rs6660775	154,538,554	3.9E-21	<0.25
rs2317230	1	157,674,997	*FCRL5*	rs3761959	157,669,278	1.7E-09	0.87	rs6427386	157,530,097	9.8E-198	<0.25
			FCRL3	rs7528684	157,670,816	9.8E-198	0.87	rs2210913	157,668,993	9.8E-198	0.87
rs4656942	1	160,831,048	*LY9*	rs4656942	160,831,048	2.7E-96	1.00	rs576334	160,797,514	5.8E-195	<0.25
rs72717009	1	161,405,053	*SDHC*	rs12731669	161,410,458	5.5E-05	0.97	rs16832871	161,335,758	1.4E-142	<0.25
			FCGR2B	rs12731669	161,410,458	4.2E-83	0.97	rs6674499	161,618,151	9.8E-198	<0.25
rs17668708	1	198,640,488	*PTPRC*	rs17669032	198,653,174	5.2E-05	0.97	rs2296618	198,666,232	2.1E-05	0.78
rs1980422	2	204,610,396	*CD28*	rs1980421	204,610,004	7.3E-18	1.00	rs2140148	204,572,140	8.1E-21	0.47
rs10028001	4	79,502,972	*ANXA3*	rs10028001	79,502,972	1.1E-04	1.00	rs4975144	79,474,040	1.4E-09	<0.25
rs2561477	5	102,608,924	*PAM*	rs411648	102,602,902	2.2E-113	1.00	rs2431321	102,118,794	9.8E-198	<0.25
			GIN1	rs2288786	102,600,754	1.3E-06	1.00	rs42431	102,400,063	2.6E-13	0.43
rs657075	5	131,430,118	*ACSL6*	rs657075	131,430,118	3.8E-12	1.00	rs253946	131,330,461	9.2E-26	0.32
chr6:14103212	6	14,103,212	*CD83*	rs12530098	14,107,197	2.6E-24	1.00	rs16874672	14,087,484	2.2E-26	0.90
			KCTD20	rs4713969	36,349,008	8.2E-05	0.99	rs4711453	36,439,391	3.1E-32	<0.25
rs2234067	6	36,355,654	*STK38*	rs4713969	36,349,008	1.4E-06	0.99	rs1812018	36,557,976	6.8E-15	<0.25
			-	rs4713969	36,349,008	2.1E-26	0.99	rs10947614	36,573,822	1.1E-146	<0.25
			SFRS3	rs4713969	36,349,008	2.6E-11	0.99	rs7743396	36,579,252	1.5E-52	<0.25
rs9373594	6	149,834,574	*C6orf72*	rs9377224	149,853,707	4.0E-06	1.00	rs9322189	149,909,933	1.8E-15	0.30
			NUP43	rs9377224	149,853,707	4.1E-64	1.00	rs9688350	150,052,113	9.8E-198	0.27
rs2451258	6	159,506,600	*RSPH3*	rs2485363	159,506,121	5.0E-05	1.00	rs12216499	159,368,524	2.0E-119	<0.25
rs1571878	6	167,540,842	*RNASET2*	rs1571878	167,540,842	9.8E-198	1.00	rs429083	167,383,972	9.8E-198	0.39
			TNPO3	rs3807306	128,580,680	1.4E-150	0.81	rs3807306	128,580,680	1.4E-150	0.81
chr7:128580042	7	128,580,042	-	rs3807306	128,580,680	2.4E-32	0.81	rs10229001	128,599,397	4.5E-49	0.48
			IRF5	rs3807306	128,580,680	9.8E-198	0.81	rs7807018	128,640,188	9.8E-198	0.48
rs2736337	8	11,341,880	*C8orf13,C8orf12*	rs2736340	11,343,973	1.6E-174	0.99	rs4840568	11,351,019	3.8E-175	0.92
			BLK	rs1478901	11,347,833	1.8E-120	0.99	rs998683	11,353,000	1.5E-120	0.95
			TRAF1	rs10985070	123,636,121	3.9E-72	1.00	rs2416804	123,676,396	3.8E-73	0.96
rs10985070	9	123,636,121	*PHF19*	rs10985070	123,636,121	2.9E-10	1.00	rs10760129	123,700,183	2.2E-10	0.95
			C5	rs10985070	123,636,121	4.9E-68	1.00	rs2416811	123,789,634	2.0E-146	0.31
rs947474	10	6,390,450	-	rs947474	6,390,450	6.5E-06	1.00	rs12416248	6,391,031	1.1E-43	<0.25
rs2671692	10	50,097,819	*WDFY4*	rs2671692	50,097,819	3.0E-09	1.00	rs7072606	49,933,974	1.1E-50	<0.25
			C11orf10	rs968567	61,595,564	3.1E-39	1.00	rs174538	61,560,081	2.5E-67	0.40
rs968567	11	61,595,564	*FADS1*	rs968567	61,595,564	8.1E-62	1.00	rs968567	61,595,564	8.1E-62	1.00
			FADS2	rs968567	61,595,564	4.8E-34	1.00	rs968567	61,595,564	4.8E-34	1.00
rs10774624	12	111,833,788	*SH2B3*	rs653178	112,007,756	1.7E-19	0.86	rs2239195	111,881,309	1.0E-33	<0.25
			ALDH2	rs653178	112,007,756	8.7E-07	0.86	rs16941669	112,245,637	4.4E-50	<0.25
rs4780401	16	11,839,326	*TXNDC11*	rs11075010	11,828,013	8.3E-09	0.93	rs12919035	11,821,508	4.4E-12	0.49
			ZNF594	rs8080217	5,164,761	8.7E-11	0.88	rs2071466	5,031,946	1.5E-12	0.65
			C17orf67	rs8080217	5,164,761	3.3E-05	0.88	rs2641232	5,087,602	1.4E-53	<0.25
rs72634030	17	5,272,580	-	rs8080217	5,164,761	3.6E-70	0.88	rs7426	5,288,983	9.8E-198	<0.25
			NUP88	rs8080217	5,164,761	3.3E-27	0.88	rs1989946	5,313,152	8.9E-96	<0.25
			MIS12	rs8080217	5,164,761	8.5E-10	0.88	rs1805448	5,384,327	2.2E-35	<0.25
			FBXL20	rs12937013	37,665,571	3.4E-15	1.00	rs8076462	37,400,025	3.1E-42	<0.25
rs1877030	17	37,740,161	*PPP1R1B*	rs1877030	37,740,161	1.8E-10	1.00	rs879606	37,781,849	8.0E-18	0.41
			-	rs11657058	37,699,378	3.9E-05	1.00	rs7219814	37,478,801	2.1E-111	<0.25
			IKZF3	rs4795385	37,733,148	8.8E-24	1.00	rs2517955	37,843,681	5.2E-82	0.33
			-	rs907092	37,922,259	6.6E-11	0.90	rs7219814	37,478,801	2.1E-111	<0.25
chr17:38031857	17	38,031,857	*IKZF3*	rs11557467	38,028,634	3.3E-05	0.84	rs9896940	37,895,975	3.1E-25	<0.25
			GSDMB	rs10852936	38,031,714	9.8E-198	0.98	rs9901146	38,043,343	9.8E-198	0.84
			ORMDL3	rs10852936	38,031,714	9.8E-198	0.98	rs8076131	38,080,912	9.8E-198	0.86
rs2469434	18	67,544,046	*CD226*	rs1610555	67,543,147	2.3E-33	0.99	rs763361	67,531,642	2.4E-50	0.66
rs4239702	20	44,749,251	*CD40*	rs4239702	44,749,251	1.3E-34	1.00	rs745307	44,747,086	1.5E-72	<0.25
			IL10RB	rs11702844	34,759,876	1.3E-11	0.97	rs1058867	34,669,381	3.0E-69	<0.25
rs73194058	21	34,764,288	*IFNAR1*	rs11702844	34,759,876	8.0E-12	0.97	rs2257167	34,715,699	4.2E-73	<0.25
			TMEM50B	rs11702844	34,759,876	3.1E-11	0.97	rs1059293	34,809,693	2.2E-103	<0.25
			-	rs11702844	34,759,876	2.8E-34	0.97	rs2834217	34,822,150	9.8E-198	<0.25
rs1893592	21	43,855,067	*UBASH3A*	rs1893592	43,855,067	6.4E-92	1.00	rs1893592	43,855,067	6.4E-92	1.00
rs2236668	21	45,650,009	*ICOSLG*	rs7278940	45,648,992	3.7E-06	1.00	rs3788111	45,668,171	8.4E-16	<0.25
rs11089637	22	21,979,096	-	rs11089637	21,979,096	9.8E-198	1.00	rs5754217	21,939,675	9.8E-198	0.87
rs909685	22	39,747,671	*SYNGR1*	rs909685	39,747,671	1.0E-140	1.00	rs909685	39,747,671	1.0E-140	1.00
			MAP3K7IP1	rs909685	39,747,671	1.3E-05	1.00	rs5750824	39,830,123	5.9E-07	0.28

b

SNP	Chr.	Position (bp)	eQTL gene	Nominal *P* for cis-eQTL	
				$CD4^+$ T-cell	$CD14^+16^-$ Monocyte
rs28411352	1	38,278,579	*INPP5B*	0.022	**3.6E-16**
			FHL3	0.081	**8.9E-13**
rs2317230	1	157,674,997	*FCRL3*	**3.5E-06**	0.87
rs9653442	2	100,825,367	*AFF3*	**5.2E-08**	0.18
rs7731626	5	55,444,683	*IL6ST*	**2.3E-07**	0.0087
			ANKRD55	**4.1E-14**	0.43
rs2234067	6	36,355,654	*ETV7*	2.9E-04	**1.1E-10**
rs9373594	6	149,834,574	*NUP43*	5.4E-04	**1.5E-05**
rs1571878	6	167,540,842	*RNASET2*	**6.9E-20**	**1.3E-05**
rs67250450	7	28,174,986	*JAZF1*	**3.6E-17**	2.0E-04
chr7:128580042*	7	128,580,042	*TNPO3*	1.0E-04	**3.0E-07**
			MEGF9	**3.3E-06**	0.10
rs10985070	9	123,636,121	*PSMD5*	0.017	**1.8E-05**
			PHF19	0.0016	**5.6E-06**
rs968567	11	61,595,564	*FADS2*	**1.4E-31**	**8.9E-35**
			FADS1	**2.1E-32**	0.094
rs11605042	11	72,411,664	*STARD10*	0.82	**1.0E-07**
rs4409785	11	95,311,422	*SESN3*	**1.5E-11**	0.43
rs773125	12	56,394,954	*SUOX*	0.27	**1.1E-09**
rs1633360	12	58,108,052	*TSPAN31*	0.13	**1.0E-05**
			METTL21B	**1.4E-09**	**4.0E-10**
rs9603616	13	40,368,069	*COG6*	0.0011	**1.2E-05**
rs4780401	16	11,839,326	*TXNDC11*	**1.3E-05**	0.62
rs72634030	17	5,272,580	*MIS12*	0.0039	**1.3E-05**
rs1877030	17	37,740,161	*STARD3*	0.048	**4.5E-05**
			GSDMA	**2.1E-06**	0.63
chr17:38031857†	17	38,031,857	*GSDMB*	**4.3E-11**	0.19
			ORMDL3	**6.8E-09**	0.0098
rs4239702	20	44,749,251	*CD40*	0.31	**1.7E-08**
rs73194058	21	34,764,288	*IFNGR2*	0.096	**1.9E-06**
			TMEM50B	**7.5E-07**	0.013
rs1893592	21	43,855,067	*UBASH3A*	**3.8E-14**	0.92

a, *cis*-eQTL of PBMCs in the RA risk SNPs. Significant *cis*-eQTLs of RA risk SNPs is indicated (FDR $q < 0.05$). SNPs and positions are based on the positive strand of NCBI build 37. Linkage disequilibrium of the proxy SNPs evaluated in the eQTL study and the best *cis*-eQTL SNP in the region with the RA risk SNPs is indicated as r^2 values. When the expression probe was not assigned to any genes, the eQTL gene is labelled with a dash. **b**, *cis*-eQTL of T cells and monocytes in the RA risk SNPs. Significant *cis*-eQTLs of RA risk SNPs are indicated in bold (gene-based permutation $P < 0.05$).

* *cis*-eQTL of the proxy SNP (rs3807307, $r^2 = 0.96$) was evaluated.

† *cis*-eQTL of the proxy SNP (rs11557466, $r^2 = 0.98$) was evaluated.

Lupus (2014) 23, 1435–1442
http://lup.sagepub.com

LUPUS AROUND THE WORLD

A nationwide study of SLE in Japanese identified subgroups of patients with clear signs patterns and associations between signs and age or sex

C Terao[1,2], R Yamada[1], T Mimori[2], K Yamamoto[3] and T Sumida[4]
[1]Center for Genomic Medicine; [2]Department of Rheumatology and Clinical Immunology, Kyoto University Graduate School of Medicine, Kyoto, Japan; [3]Department of Allergy and Rheumatology, Graduate School of Medicine, University of Tokyo, Tokyo, Japan; and [4]Department of Internal Medicine, Faculty of Medicine, University of Tsukuba, Ibaraki, Japan

We performed a nationwide study to determine the distributions of the signs and clinical markers of systemic lupus erythematosus (SLE) and identify any patterns in their distributions to allow patient subclassification. We obtained 256,999 patient-year records describing the disease status of SLE patients from 2003 to 2010. Of these, 14,779 involved patients diagnosed within the last year, and 242,220 involved patients being followed up. Along with basic descriptive statistics, we analyzed the effects of sex, age and disease duration on the frequencies of signs in the first year and follow-up years. The patients and major signs were clustered using the Ward method. The female patients were younger at onset. Renal involvement and discoid eczema were more frequent in males, whereas arthritis, photosensitivity and cytopenia were less. Autoantibody production and malar rash were positively associated with young age, and serositis and arthritis were negatively associated. Photosensitivity was positively associated with a long disease duration, and autoantibody production, serositis and cytopenia were negatively associated. The SLE patients were clustered into subgroups, as were the major signs. We identified differences in SLE clinical features according to sex, age and disease duration. Subgroups of SLE patients and the major signs of SLE exist. *Lupus* (2014) **23,** 1435–1442.

Key words: Systemic lupus erythematosus; anti-dsDNA antibodies; anticardiolipin; antibodies; hematologic changes; renal lupus; musculoskeletal

Introduction

Systemic lupus erythematosus (SLE) is an autoimmune disorder that involves multiple organs and can lead to severe complications including cerebral infarction, myocardial infarction, infection, renal failure and a poor prognosis.[1–4] SLE is characterized by the heterogeneity of its clinical features, and we have yet to fully understand this heterogeneity, which is one of the reasons why classification criteria for SLE[5] were developed, and new criteria were recently proposed.[6]

Correspondence to: Ryo Yamada, Center for Genomic Medicine, Kyoto University Graduate School of Medicine, Shogoin Kawahara, Kyoto 606-8507, Japan.
Email: ryamada@genome.med.kyoto-u.ac.jp
Received 10 December 2013; accepted 25 July 2014

Epidemiological studies of SLE

Epidemiological studies of SLE can be classified into two types. The first type involves studies on relatively detailed issues, including the clinical features of SLE, that included only a limited number of patients. The second type involves studies on limited epidemiological indices, such as the incidence and prevalence of the condition, that included many registrants. Most of the first type of studies were hospital-, clinic- or limited region-based studies with fewer than 1000 SLE patients,[7–11] although some of these studies recruited participants from multiple regions within a nation.[12] There have been only two national registry-based studies of SLE, which were performed in Taiwan and Japan.[13,14] The sample sizes of these two studies were 22,182 and 21,405, respectively. SLE is three to 10 times more common in females than in males.[15] The age at onset of SLE peaks from 15 to 30, and the female:male ratio has been reported to be highest

10.1177/0961203314547790

in individuals of reproductive age and decreases in adolescence and old age.[16] While some European studies have reported differences in the age at onset between males and females,[17] a relatively large study involving 1790 cases from China did not detect a significant difference in the mean onset age between the sexes.[18] Thus, it is unclear whether there is no difference in the onset age of SLE between males and females or whether such differences are observed only in patients of European descent.

Signs and clinical markers of SLE

SLE produces a wide range of clinical signs, including physical signs and laboratory findings. Various reports have detected associations between the clinical features of SLE and age/sex, either at disease onset or throughout the clinical course of the condition. Thus, these reports suggested that age and/or sex can affect the signs of SLE. Efforts have been made to identify subgroups of SLE based on clinical manifestations.[19,20] However, limited power of previous reports made it difficult to draw conclusions. A detailed analysis of the clinical features of SLE in a large-scale study would increase our understanding of the clinical heterogeneity of SLE.

Here, we performed a nationwide surveillance study of patients with SLE in Japan to characterize the epidemiological and clinical features of SLE. As far as we know, this is the largest such study to have ever been conducted.

Patients and methods

SLE patient registration

In Japan, a total of 56 diseases are defined as "Nanbyo (intractable disease)" and patients are given a questionnaire about their clinical status and history, which is filled out by the clinician providing their care, during registration. The clinicians are not limited to specialists for the diseases. The registered information is used for making decisions by experts on the public financial support provided for their medical care. Each patient is enrolled as a new registrant in the first year after diagnosis, and his or her registration is renewed annually by different forms from the first ones (follow-up registry). SLE is one of these "Nanbyo." This registry-based financial support system is well known throughout the country, and Japanese public health departments and health care professionals believe that the vast majority of patients with the diseases that receive medical care are registered annually. Clinical information in the questionnaire for the SLE forms is listed in Supplementary Table 1.

We obtained text files electronically converted from nationwide registry data about SLE in Japan from 2003 to 2010.[14] Although the text files did not cover all the registrants, in total, 14,779 new registries were obtained from 2003 to 2010 and we adopted 2009 (44,249 patients), which covered the largest parts of the annual total registries (81.2%) as a year with representative follow-up data after we found that each year's follow-up registries displayed similar basic statistics. For new registries, we omitted suspected duplicate registries and identified 14,030 registrants as novel for the purposes of this study. We extracted 9374 registries for which information about disease onset was available and for which it could be confirmed that disease onset had occurred within the last year. Schematic images of quality control of the dataset were illustrated in Supplementary Figure 1. We evaluated two patient groups; the first group, which was collected from 2003 to 2010, consisted of patients who had been diagnosed with SLE within the last year, and the other group consisted of all patients in the representative year, 2009. We called these two groups the "novel SLE" and "all SLE" groups, respectively.

Clinical information

We extracted information about the patients' clinical features including the 11 major signs included in the American College of Rheumatology (ACR) classification,[5] age, sex, age at diagnosis, and complications (infection, bone necrosis, compression fracture of bone, gastric ulcers, myocardial infarction and cerebral infarction) from the registry for all registrants. Some items, including information about antinuclear antibody (ANA) positivity, anti-Smith (anti-Sm) antibody positivity, anti-double-stranded DNA (anti-dsDNA) antibody positivity, the occurrence of biological false-positives on the syphilis test, lupus anti-coagulant positivity and anticardiolipin antibody positivity, were available only for the novel group (Supplementary Table 1).

Sex ratio

The female:male ratio was estimated in the all SLE group.

Age distribution of SLE patients

Age at onset was compared between males and females in the novel SLE and all SLE groups.

The significance of the difference was tested by logistic regression analysis.

Analysis of SLE signs and clinical markers in patients with SLE

The frequencies of SLE signs and clinical markers were analyzed in the novel and all SLE groups. The effects of age, sex and disease duration were assessed separately and in combination by multiple logistic regression analysis. Clustering of the major signs and patients was performed in 6637 patients in the novel SLE group for whom data regarding the 11 major signs and clinical markers were available and 10,000 randomly selected patients in the all SLE group for whom data regarding the 10 major signs and clinical markers other than ANA were available (Supplementary Figure 1). The associations between complications and the patients' basic information, SLE signs and clinical markers were also analyzed. We regarded autoantibody positivity at any point during the disease course as positivity.

Statistical analysis

Statistical analyses were performed using the R or SPSS (ver18) software.

Results

Female ratio of SLE

The female:male ratio was 8.14 in the all SLE group and was comparable to those described in previous reports (8.1–12.5).[21–23] A comparison of the age distributions of the male and female SLE patients in the all SLE group showed that the females were younger than the males ($p = 0.00031$, Figure 1(a)). The females were also younger at onset than the males ($p = 4.1 \times 10^{-62}$, Figure 1(b)).

Prevalence of clinical features and the effects of age and sex on them in the all SLE group

The prevalence of the 10 major signs of SLE (as outlined by the ACR, except for ANA positivity) varied (Figure 2(a), Supplementary Table 2). Cytopenia and arthritis were the two most common signs, and serositis was the least common sign. The frequencies of some of the 10 SLE signs differed markedly between males and females (Figure 2(b)). An analysis of the effects of age on the frequencies of these signs revealed four patterns: increases with age, decreases with age, a U-shaped age distribution (lowest in middle aged subjects), and an inverse-U shaped age distribution (highest in middle-aged subjects) (Figure 2(c)). An analysis of the effects of disease duration on the frequencies of these signs revealed that most of them were frequently observed in the short duration after onset. The signs' disease duration-based frequency patterns were similar to their age-based patterns. Photosensitivity was the only sign associated with a long disease duration (Figure 2(d)). Discoid eczema was the only sign that was not associated with disease duration. The detailed results are shown in Supplementary Figure 2 and Supplementary Table 3, and further analyses of the detailed signs of SLE are shown in the Supplementary notes and Supplementary Figure 3.

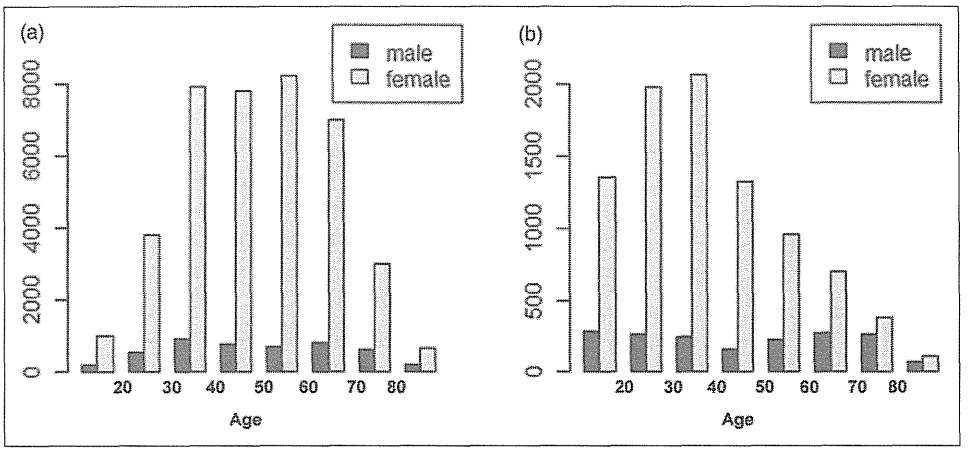

Figure 1 Distribution of patients who developed systemic lupus erythematosus (SLE). (a) Distribution of the current ages of the SLE patients. (b) Distribution of the age at onset of the SLE patients.

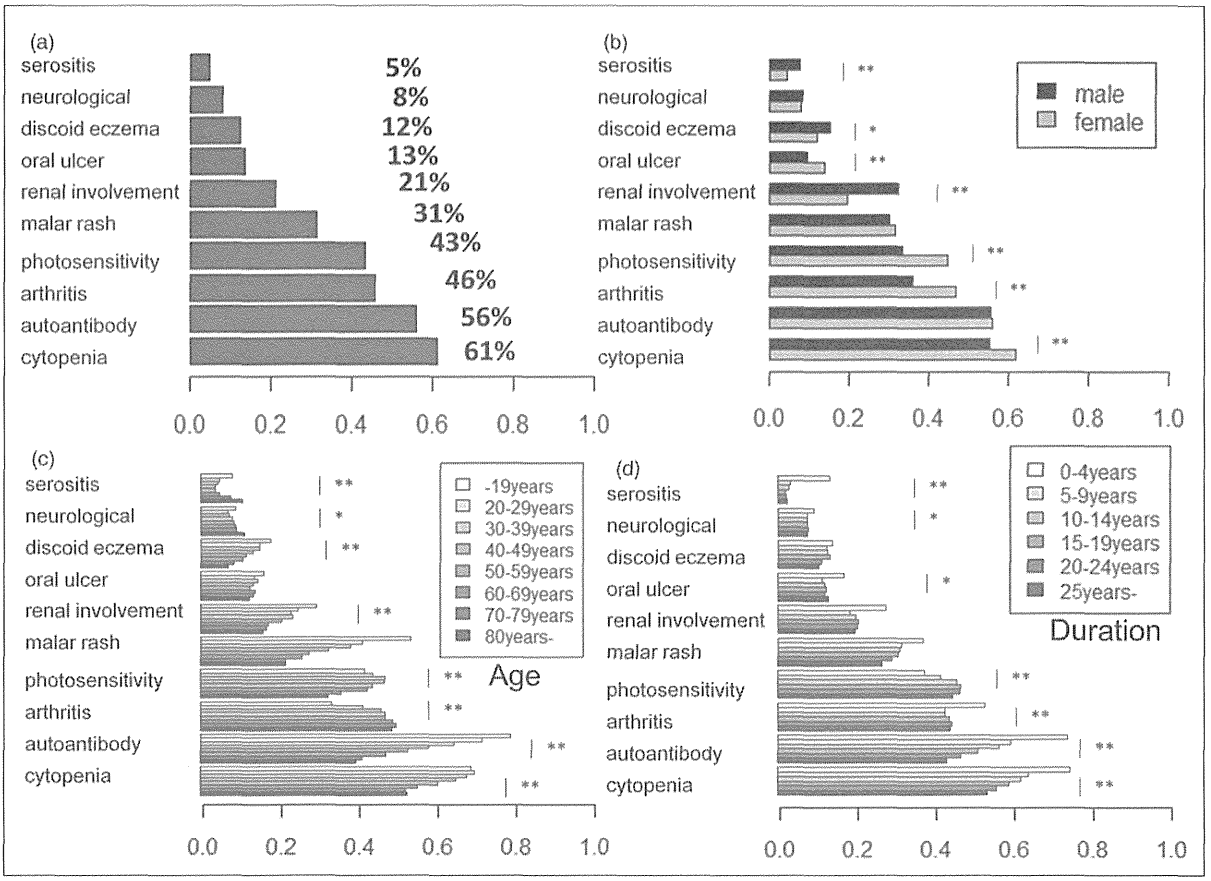

Figure 2 Distribution and clusters of systemic lupus erythematosus (SLE) signs and patients in the all SLE group. (a) Frequency of SLE signs in a year. Frequencies of SLE signs according to sex (b), age (c) and disease duration (d). *p value $<10^{-5}$, **p value $<10^{-10}$.

Prevalence of signs and clinical markers and the effects of age and sex on them in the novel SLE group

The prevalence of the major signs of SLE also varied in the novel SLE patients, and the order of the signs' frequencies (i.e. from highest to lowest) was different from that observed in the all SLE group (Figure 3(a) and Supplementary Table 2). Except for cytopenia, all of the SLE major signs were affected by sex in the same manner as was observed in the all SLE group according to multiple logistic regression analysis (Figures 2(b) and 3(b) and Supplementary Figure 4(a)). The associations between age and the SLE signs differed between the novel and all SLE groups for four of the 10 items (Figures 2(c) and 3(c) and Supplementary Figure 4). Two patterns of difference were observed. The first type involved a positive association with age being observed only in the novel SLE group. The other type involved a positive association with age not being observed in the novel SLE group. Oral ulcers exhibited the former pattern ($p = 3.9 \times 10^{-6}$), and renal involvement, cytopenia and arthritis displayed the latter pattern ($p > 0.019$). Sex-specific age associations showed a third pattern: opposite associations in the novel and all SLE groups. Namely, cytopenia was associated with old age in the males belonging to the novel SLE group, while it was associated with young age in the males in the all SLE group. In addition, three signs showed specific associations with age in the novel SLE group. The frequency of serositis increased age-dependently, whereas the frequencies of renal involvement and arthritis showed U and inverse-U patterns, respectively. The detailed results of the analyses and further analyses are shown in the Supplementary notes and Supplementary Table 4.

Clustering analysis of the coexistence of signs and clinical markers in the all SLE and novel SLE groups

Clustering analysis of the 11 signs in the patients in the novel SLE group revealed that they could be

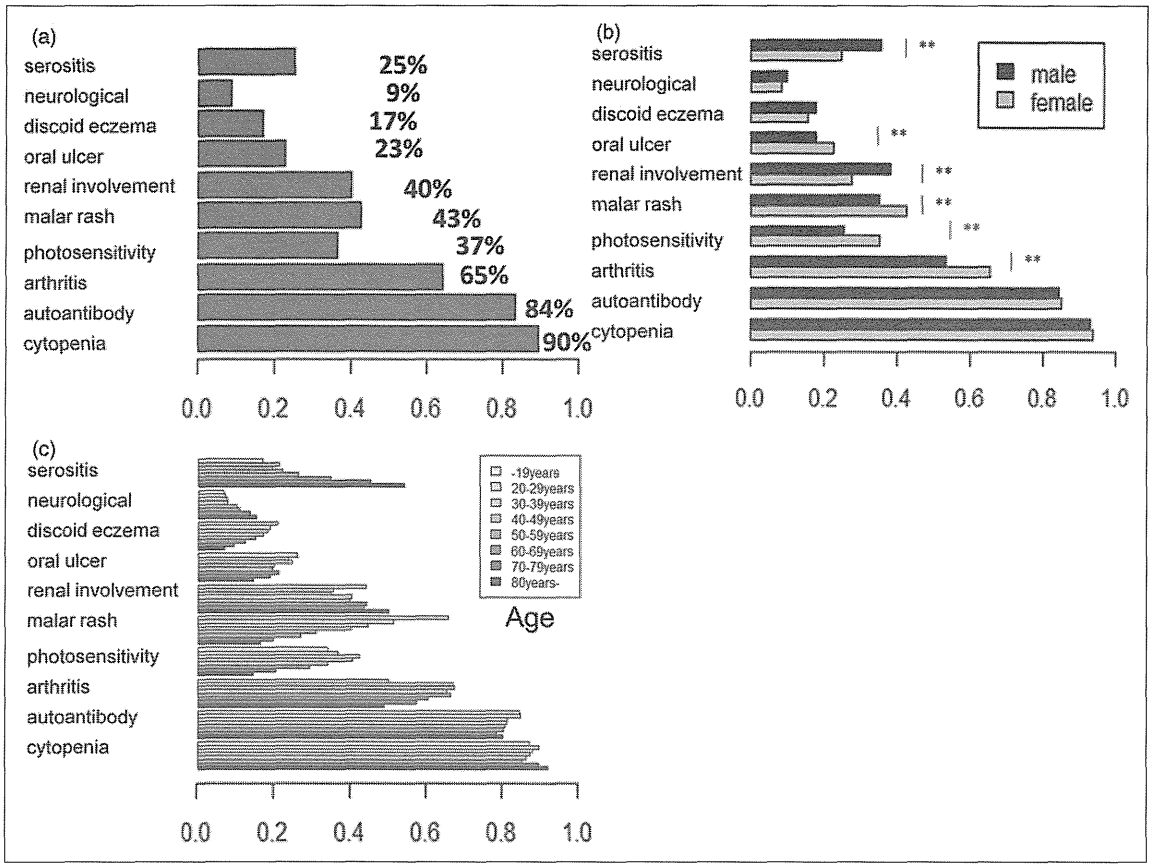

Figure 3 Distribution and clusters of systemic lupus erythematosus (SLE) signs and patients in the novel SLE group. (a) Frequencies of SLE signs during the first year after diagnosis. Frequency of SLE signs within a year of diagnosis according to sex (b) and age (c) based on multiple logistic linear regression analysis. *p value $<10^{-5}$, **p value $<10^{-10}$.

divided into two groups; namely, a group containing autoantibody positivity, ANA positivity, cytopenia and arthritis, and another group including the other seven signs and markers (Figure 4(a)). The novel SLE patients (6637) were also subjected to clustering analysis, which showed that they could be classified into 10 clusters according to their signs (Figure 4(b)). The sign frequencies and the numbers of SLE patients in each cluster are shown in Supplementary Table 5.

Cluster analysis of the 10 major SLE signs (not including ANA) in the all SLE group showed that they could be subgrouped into two clusters with the similar characteristics as those observed in the analysis of the novel SLE group although differences were observed among the finer cluster divisions (Figure 4(c)). Cluster analysis of 10,000 randomly selected SLE patients from the all SLE group produced eight clear clusters (Figure 4(d) and Supplementary Table 6). The patterns of clusters partly matched those observed in the novel SLE group.

Further analyses: complications of SLE and the distributions of specific autoantibodies

The complications of SLE were also assessed in the all SLE group, as were the effects of age, sex and disease duration. The associations of autoantibodies with complications were assessed according to age, sex and disease duration to assess their utility as predictive markers. The associations between complications and each SLE patient cluster were also analyzed. See the Supplementary notes for details.

Discussion

Although some small studies did not report a significant difference in age at onset between the sexes,[18] our large-scale study demonstrated that female patients developed SLE at a younger age than male patients. We evaluated the clinical features of two patient populations, "the novel

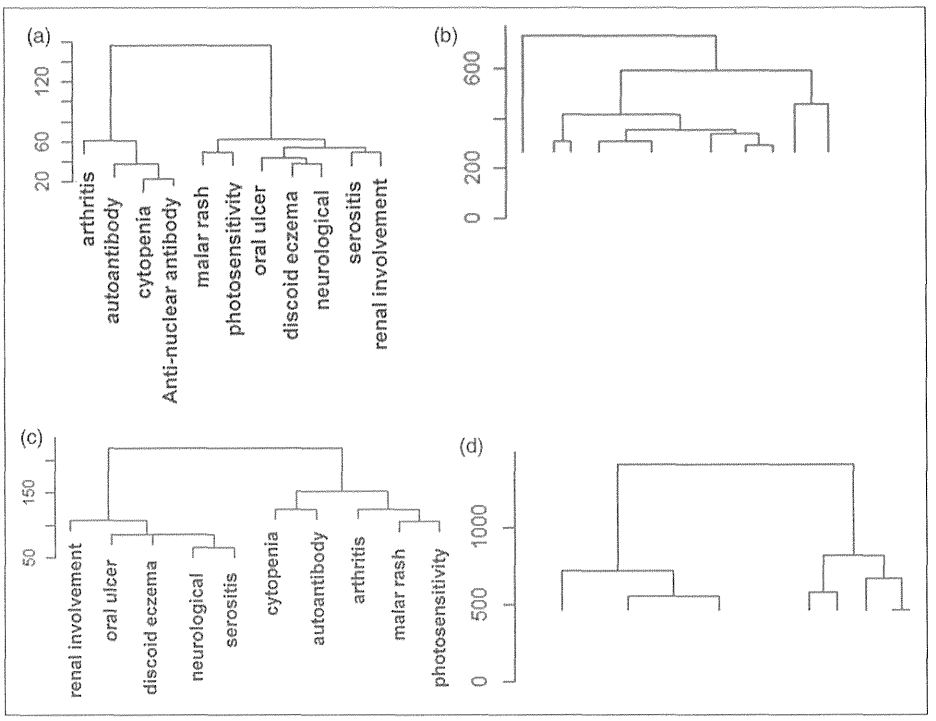

Figure 4 Clusters of systemic lupus erythematosus (SLE) signs and patients. (a) Clustering of 11 SLE major signs in patients who had been diagnosed with SLE within the last year. (b) Clustering of 6637 SLE patients who had been diagnosed with SLE within the last year. (c) Clustering of 10 major SLE signs in the all SLE group. (d) Clustering of 10,000 SLE patients in the all SLE group.

patients": i.e. patients who had been diagnosed with SLE within the last year, and "all patients": i.e. all patients regardless of their disease duration. As a result, we obtained evidence of associations between SLE signs and age, sex and disease duration. In our study, the frequencies of 11 major signs were similar to those obtained in previous reports from Asian and European countries both in the novel SLE and all SLE groups with the exception of serositis (25.3% in the novel SLE group, 4.6% in the all SLE group; 5%–22% at onset and 20%–40% prevalence in previous studies).[18,23–27] This difference might have been due to the relative difficulty of detecting serositis compared with other features.

We validated previous reports of higher frequencies of serositis,[28,29] renal involvement[29,30] and discoid eczema[29–31] in males and higher frequencies of photosensitivity[30] and oral ulcers[30] in females. Although neurological involvement was reported to be more common in males in two previous reports,[32,33] our study did not find any difference between the sexes. The difference between the sexes in the frequency of malar rash is disputed, and our study did not detect any sex difference. Our results indicate that any inter-sex difference in neurological involvement and malar rash is very small. The sex difference in the frequency of arthritis is also disputed, and we observed a significantly higher frequency of arthritis in females (47.0% in females and 36.0% in males with $p = 1.3 \times 10^{-44}$).

Only a few previous studies comprising more than 500 patients have examined the effects of age on the clinical manifestations of SLE.[18,28,34,35] Previous studies reported positive associations of younger age with malar rash, discoid eczema, autoantibody production and photosensitivity,[18,30] and we confirmed these associations. In addition, we demonstrated that serositis and neurological involvement were positively associated with older age. Renal involvement was associated with younger age only in the novel SLE group.

No studies have ever analyzed the detailed effects of disease duration on SLE signs. Most of the major signs and clinical markers of SLE, especially serositis, displayed higher prevalence in the patients with short disease durations. Only the prevalence of photosensitivity increased according to disease duration. Discoid eczema was not associated with disease duration.

We performed similar analyses for more detailed signs of SLE (Supplementary notes).

The 11 SLE signs were classified into two groups according to their manifestation patterns in the novel SLE group: group 1 (ANA, autoantibody positivity (anti-Sm antibody and anti-dsDNA antibody), cytopenia, and arthritis) and group 2 (malar rash, discoid eczema, photosensitivity, oral ulcers, neurological involvement, serositis and renal involvement). The first group included hematoserological abnormalities such as cytopenia and arthritis was considered to be an inflammatory/autoimmunity-related reaction and so was classified with the hematoserological abnormalities because of its reduced organ specificity compared to the items in group 2. Therefore, we called group 1 the hematoserological group and group 2 the organ-specific group. In the all SLE group, such clear clustering was not very apparent, which might have been because individual patients tended to present with various features during their clinical courses.

The SLE patients in the novel SLE group were clustered into 10 groups according to the signs that they displayed. These groups were not associated with sex or age (analysis of variance (ANOVA), data not shown). At onset, the frequencies of the 10 groups ranged from 4.0% to 22.4%. The 10 groups were characterized as: represented by (1) neurological involvement (22.4%), (2) discoid eczema (10.6%), (3) a lack of autoantibodies other than ANA (12.7%), (4) oral ulcers (9.1%), (5) renal involvement (9.9%), (6) photosensitivity (5.7%), (7) a lack of arthritis (6.5%), (8) serositis (9.8%), (9) malar rash (4.0%) and (10) others (9.3%). It should be noted that each group was represented by one of the items in the organ-specific group or a lack of an item in the hematoserological group. These findings suggest that the items in the organ-specific group are the predominant determinants of a patient's condition. In the all SLE group, eight clusters, which displayed frequencies ranging from 3.9% to 31.5%, were determined. The clusters were characterized as follows: 1) no signs or markers (6.9%), 2) cytopenia alone (5.1%), 3) autoantibody positivity alone (3.9%), 4) cytopenia and autoantibody positivity only (5.9%), 5) arthritis (9.1%), 6) renal involvement (16.4%), 7) neurological signs and serositis (21.3%) and 8) others (31.5%). The novel SLE and all SLE groups shared two clusters with similar characteristics, i.e. the "neurological signs" and "renal involvement" clusters. The reduced frequencies of signs and clinical markers observed in the all SLE group led to clusters based on one or no signs. The lack of information about ANA during the chronic phase might also have reduced the number of clusters. We performed five rounds of resampling, each of which involved 10,000 patients, and the same clusters were maintained (data not shown). These results confirm that SLE patients and signs can be subgrouped into clear clusters. However, the 11 or 10 signs of SLE could not consistently explain the division of clusters among different stages of the disease. This raised the possibility that underlying factors related to the pathology of SLE other than the 11 signs exist. While we analyzed the associations between clusters and clinical signs or complications, we could not analyze the association between clusters and death because of a lack of information. Although the follow-up questionnaire included information about death causes (data not shown), this information was not filled out in most cases. This could be explained by the system of the nationwide study in which patients ask physicians to fill out the questionnaire. Associations between clusters in all SLE group and some complications (Supplementary notes) suggest the possibility that clusters are associated with severity and prognosis of SLE. Further follow-up studies would clarify the clinical characteristics of the abovementioned clusters.

Finally, we would like to comment on our data source. As the primary purpose of the national registry is to determine whether patients qualify for public financial aid, there could be a bias toward the over-rating of the signs. Despite our concern about such overestimation, the frequencies of individual signs in our study were similar to those described in previous reports from Asian countries,[36] indicating that any over-rating was not too problematic. Considering the number of subjects analyzed in the current study and the fact that the same tendencies were observed during each year (data not shown), our results regarding the patterns of signs and the associations between these signs and gender, age and disease duration in Japanese SLE patients should be regarded as conclusive.

In conclusion, we have obtained conclusive evidence about the distributions of the clinical features of SLE and their relationships with sex, age and age at onset.

Funding

This work was supported by grants-in-aid from the Ministry of Health, Labor, and Welfare of Japan.

Conflict of interest statement

The authors have no conflicts of interest to declare.

References

1 Tsokos GC. Systemic lupus erythematosus. *N Engl J Med* 2011; 365: 2110–2121.
2 Bengtsson C, Ohman ML, Nived O, Rantapää Dahlqvist S. Cardiovascular event in systemic lupus erythematosus in northern Sweden: Incidence and predictors in a 7-year follow-up study. *Lupus* 2012; 21: 452–459.
3 Murray SG, Yazdany J, Kaiser R, *et al.* Cardiovascular disease and cognitive dysfunction in systemic lupus erythematosus. *Arthritis Care Res (Hoboken)* 2012; 64: 1328–1333.
4 Chiu CC, Huang CC, Chan WL, *et al.* Increased risk of ischemic stroke in patients with systemic lupus erythematosus: A nationwide population-based study. *Intern Med* 2012; 51: 17–21.
5 Hochberg MC. Updating the American College of Rheumatology revised criteria for the classification of systemic lupus erythematosus. *Arthritis Rheum* 1997; 40: 1725.
6 Petri M, Orbai AM, Alarcón GS, *et al.* Derivation and validation of the Systemic Lupus International Collaborating Clinics classification criteria for systemic lupus erythematosus. *Arthritis Rheum* 2012; 64: 2677–2686.
7 Ward MM. Prevalence of physician-diagnosed systemic lupus erythematosus in the United States: Results from the third national health and nutrition examination survey. *J Womens Health (Larchmt)* 2004; 13: 713–718.
8 Amor B, Bouchet H, Delrieu F. National survey on reactive arthritis by the French Society of Rheumatology [article in French]. *Rev Rhum Mal Osteoartic* 1983; 50: 733–743.
9 Gudmundsson S, Steinsson K. Systemic lupus erythematosus in Iceland 1975 through 1984. A nationwide epidemiological study in an unselected population. *J Rheumatol* 1990; 17: 1162–1167.
10 Somers EC, Thomas SL, Smeeth L, Schoonen WM, Hall AJ. Incidence of systemic lupus erythematosus in the United Kingdom, 1990–1999. *Arthritis Rheum* 2007; 57: 612–618.
11 Helve T. Prevalence and mortality rates of systemic lupus erythematosus and causes of death in SLE patients in Finland. *Scand J Rheumatol* 1985; 14: 43–46.
12 Hiraki LT, Feldman CH, Liu J, *et al.* Prevalence, incidence, and demographics of systemic lupus erythematosus and lupus nephritis from 2000 to 2004 among children in the US Medicaid beneficiary population. *Arthritis Rheum* 2012; 64: 2669–2676.
13 Chiu YM, Lai CH. Nationwide population-based epidemiologic study of systemic lupus erythematosus in Taiwan. *Lupus* 2010; 19: 1250–1255.
14 Ohta A, Nagai M, Nishina M, Tomimitsu H, Kohsaka H. Age at onset and gender distribution of systemic lupus erythematosus, polymyositis/dermatomyositis, and systemic sclerosis in Japan. *Mod Rheumatol* 2013; 23: 759–764.
15 Pons-Estel GJ, Alarcón GS, Scofield L, Reinlib L, Cooper GS. Understanding the epidemiology and progression of systemic lupus erythematosus. *Semin Arthritis Rheum* 2010; 39: 257–268.
16 Lahita RG. The role of sex hormones in systemic lupus erythematosus. *Curr Opin Rheumatol* 1999; 11: 352–356.
17 Lu LJ, Wallace DJ, Ishimori ML, Scofield RH, Weisman MH. Review: Male systemic lupus erythematosus: A review of sex disparities in this disease. *Lupus* 2010; 19: 119–129.
18 Feng JB, Ni JD, Yao X, *et al.* Gender and age influence on clinical and laboratory features in Chinese patients with systemic lupus erythematosus: 1,790 cases. *Rheumatol Int* 2010; 30: 1017–1023.
19 Levy DM, Peschken CA, Tucker LB, *et al.* Influence of ethnicity on childhood-onset systemic lupus erythematosus: Results from a multiethnic multicenter Canadian cohort. *Arthritis Care Res (Hoboken)* 2013; 65: 152–160.
20 Jacobsen S, Petersen J, Ullman S, *et al.* A multicentre study of 513 Danish patients with systemic lupus erythematosus. I. Disease manifestations and analyses of clinical subsets. *Clin Rheumatol* 1998; 17: 468–477.
21 Pons-Estel BA, Catoggio LJ, Cardiel MH, *et al.* The GLADEL multinational Latin American prospective inception cohort of 1,214 patients with systemic lupus erythematosus: Ethnic and disease heterogeneity among "Hispanics". *Medicine (Baltimore)* 2004; 83: 1–17.
22 Ballou SP, Khan MA, Kushner I. Clinical features of systemic lupus erythematosus: Differences related to race and age of onset. *Arthritis Rheum* 1982; 25: 55–60.
23 Wang F, Wang CL, Tan CT, Manivasagar M. Systemic lupus erythematosus in Malaysia: A study of 539 patients and comparison of prevalence and disease expression in different racial and gender groups. *Lupus* 1997; 6: 248–253.
24 Tan TC, Fang H, Magder LS, Petri MA. Differences between male and female systemic lupus erythematosus in a multiethnic population. *J Rheumatol* 2012; 39: 759–769.
25 Garcia MA, Marcos JC, Marcos AI, *et al.* Male systemic lupus erythematosus in a Latin-American inception cohort of 1214 patients. *Lupus* 2005; 14: 938–946.
26 Malaviya AN, Chandrasekaran AN, Kumar A, Shamar PN. Systemic lupus erythematosus in India. *Lupus* 1997; 6: 690–700.
27 Chahade WH, Sato EI, Moura JE Jr, Costallat LT, Andrade LE. Systemic lupus erythematosus in São Paulo/Brazil: A clinical and laboratory overview. *Lupus* 1995; 4: 100–103.
28 Cervera R, Khamashta MA, Font J, *et al.* Systemic lupus erythematosus: Clinical and immunologic patterns of disease expression in a cohort of 1,000 patients. The European Working Party on Systemic Lupus Erythematosus. *Medicine (Baltimore)* 1993; 72: 113–124.
29 Soto ME, Vallejo M, Guillén F, Simón JA, Arena E, Reyes PA. Gender impact in systemic lupus erythematosus. *Clin Exp Rheumatol* 2004; 22: 713–721.
30 Voulgari PV, Katsimbri P, Alamanos Y, Drosos AA. Gender and age differences in systemic lupus erythematosus. A study of 489 Greek patients with a review of the literature. *Lupus* 2002; 11: 722–729.
31 Font J, Cervera R, Navarro M, *et al.* Systemic lupus erythematosus in men: Clinical and immunological characteristics. *Ann Rheum Dis* 1992; 51: 1050–1052.
32 Stefanidou S, Benos A, Galanopoulou V, *et al.* Clinical expression and morbidity of systemic lupus erythematosus during a post-diagnostic 5-year follow-up: A male:female comparison. *Lupus* 2011; 20: 1090–1094.
33 Mok CC, To CH, Ho LY, Yu KL. Incidence and mortality of systemic lupus erythematosus in a southern Chinese population, 2000–2006. *J Rheumatol* 2008; 35: 1978–1982.
34 Ward MM, Polisson RP. A meta-analysis of the clinical manifestations of older-onset systemic lupus erythematosus. *Arthritis Rheum* 1989; 32: 1226–1232.
35 Lalani S, Pope J, de Leon F, Peschken C. Clinical features and prognosis of late-onset systemic lupus erythematosus: Results from the 1000 faces of lupus study. *J Rheumatol* 2010; 37: 38–44.
36 Jakes RW, Bae SC, Louthrenoo W, Mok CC, Navarra SV, Kwon N. Systematic review of the epidemiology of systemic lupus erythematosus in the Asia-Pacific region: Prevalence, incidence, clinical features, and mortality. *Arthritis Care Res (Hoboken)* 2012; 64: 159–168.

Wide-Field Fundus Autofluorescence Abnormalities and Visual Function in Patients With Cone and Cone-Rod Dystrophies

Maho Oishi, Akio Oishi, Ken Ogino, Yukiko Makiyama, Norimoto Gotoh, Masafumi Kurimoto, and Nagahisa Yoshimura

Department of Ophthalmology and Visual Sciences, Kyoto University Graduate School of Medicine, Kyoto, Japan

Correspondence: Akio Oishi, Department of Ophthalmology and Visual Sciences, Kyoto University Graduate School of Medicine, 54 Kawahara, Shogoin, Sakyo, Kyoto 606-8507, Japan; aquio@kuhp.kyoto-u.ac.jp.

Submitted: January 8, 2014
Accepted: April 4, 2014

Citation: Oishi M, Oishi A, Ogino K, et al. Wide-field fundus autofluorescence abnormalities and visual function in patients with cone and cone-rod dystrophies. *Invest Ophthalmol Vis Sci.* 2014;55:3572-3577. DOI: 10.1167/iovs.14-13912

Purpose. To evaluate the clinical utility of wide-field fundus autofluorescence (FAF) in patients with cone dystrophy and cone-rod dystrophy.

Methods. Sixteen patients with cone dystrophy (CD) and 41 patients with cone-rod dystrophy (CRD) were recruited at one institution. The right eye of each patient was included for analysis. We obtained wide-field FAF images using a ultra-widefield retinal imaging device and measured the area of abnormal FAF. The association between the area of abnormal FAF and the results of visual acuity measurements, kinetic perimetry, and electroretinography (ERG) were investigated.

Results. The mean age of the participants was 51.4 ± 17.4 years, and the mean logarithm of the minimum angle of resolution was 1.00 ± 0.57. The area of abnormal FAF correlated with the scotoma measured by the Goldman perimetry I/4e isopter ($\rho = 0.79$, $P < 0.001$). The area also correlated with amplitudes of the rod ERG ($\rho = -0.63$, $P < 0.001$), combined ERG a-wave ($\rho = -0.72$, $P < 0.001$), combined ERG b-wave ($\rho = -0.66$, $P < 0.001$), cone ERG ($\rho = -0.44$, $P = 0.001$), and flicker ERG ($\rho = -0.47$, $P < 0.001$).

Conclusions. The extent of abnormal FAF reflects the severity of functional impairment in patients with cone-dominant retinal dystrophies. Fundus autofluorescence measurements are useful for predicting retinal function in these patients.

Keywords: cone dystrophy, cone-rod dystrophy, fundus autofluorescence

Inherited retinal dystrophy is a major cause of blindness in developed countries.[1] The disease affects more than 2 million patients worldwide, and multiple causative genes have been identified.[2] Inherited retinal dystrophy can be categorized in four major groups: rod-dominant diseases, cone-dominant diseases, generalized retinal degenerations, and vitreoretinal disorders.[2] Cone dystrophy (CD) and cone-rod dystrophy (CRD) represent types of cone-dominant dystrophy.[2] Patients with panretinal cone-dominant degeneration are diagnosed with CD when rod function is preserved and diagnosed with CRD when rod function is impaired.

Rod functions are impaired relatively early in patients with CRD.[3] In addition, those who were originally diagnosed with CD can exhibit rod dysfunction once the condition has advanced.[3,4] The remaining rod photoreceptors and peripheral retinal function determine the extent of visual field loss, which is critical to a patient's quality of life.[4] Although electroretinography (ERG) is a standard technique for objectively evaluating the extent of remaining rod function, the examination is not easy to perform repeatedly in daily clinical practice.

Fundus autofluorescence (FAF) imaging is a noninvasive modality that allows the researcher to evaluate the status of photoreceptor cells and the retinal pigment epithelium. This technique can be used to visualize the distribution of lipofuscin and other fluorophores in these tissues; an increased FAF signal is thought to reflect the abnormal accumulation of fluorophores, whereas a decreased FAF signal seems to result from atrophy of the RPE.[5-7] In addition, a recent study showed that disruption of the outer retina causes increased FAF.[8] All of these changes can be associated with retinal dysfunction. In fact, previous studies reported several characteristic FAF abnormalities in inherited retinal dystrophies, such as retinitis pigmentosa,[9-15] Stargardt disease,[16-19] CD, and CRD.[19-21] However, conventional FAF imaging approaches have focused largely on the central 30-55° of the fundus due to the angle of view possible with the devices used for autofluorescence imaging. There is little available information about peripheral FAF in CD or CRD.

The Optos (Optos PLC, Dunfermline, UK) is a novel wide-field imaging device that allows for a 200° view of the retina, rendering the retinal periphery easily accessible to photography and evaluation.[22] Several studies have reported the utility of Optos technology for the evaluation of FAF in chorioretinitis,[23] retinal detachment,[24] age-related macular degeneration,[25] and retinitis pigmentosa.[13] In this study, we examined wide-field FAF images of patients with CD and CRD and compared the associated findings with other clinical parameters including visual acuity as well as the results of Goldmann perimetry (GP) and ERG.

Methods

We examined consecutive patients with CD or CRD who visited the Department of Ophthalmology and Visual Sciences, Kyoto

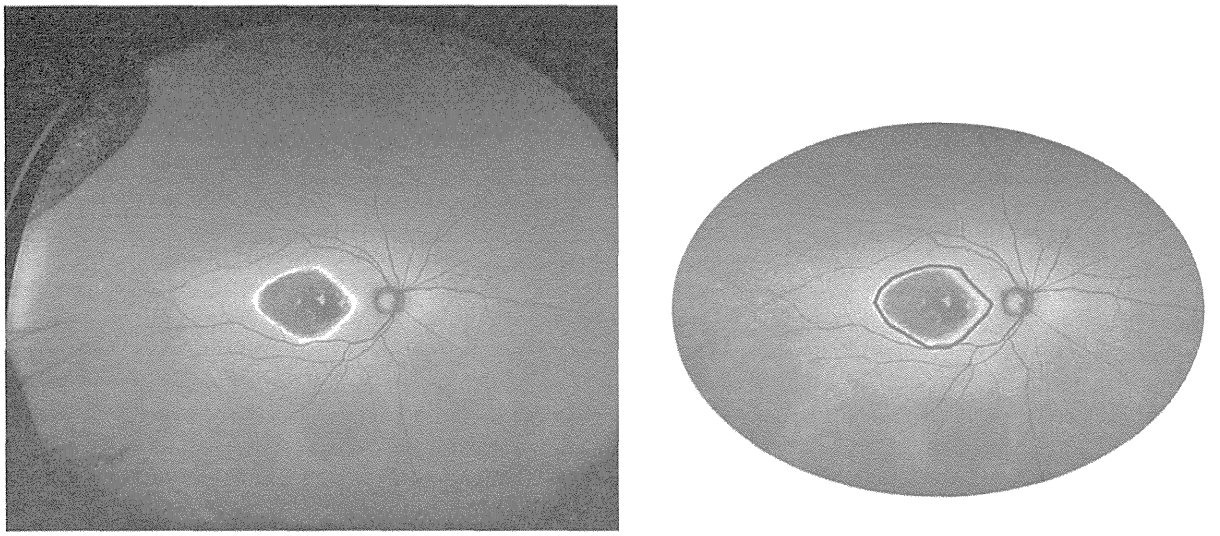

FIGURE 1. A wide-field FAF image of an eye with cone-rod dystrophy (*left*) and the measurement method employed in the present study. The measurement was done within the 3000 × 2100-pixel elliptical area. The area containing abnormal hyper- and hypo-FAF was traced, and the percentage within the elliptical area was calculated (*right*).

University Graduate School of Medicine, Kyoto, Japan during the period from March 2012 through November 2013. The protocol of the study adhered to the tenets of the Declaration of Helsinki. Approval was obtained from the Institutional Review Board (IRB)/Ethics Committee of the Kyoto University Graduate School of Medicine. The aim of the study and the measurement procedures were explained to the study participants; written informed consent was obtained from each participant.

Each patient's diagnosis was agreed upon by two retinal specialists (AO, MO). The diagnosis of CD was based on a progressive decline in visual acuity, the presence of a central scotoma, and reduced cone responses on full-field ERG, with normal rod responses. Full-field ERG was recorded according to the protocol recommended by the International Society for Clinical Electrophysiology of Vision (ISCEV) 2008.[26] Cone-rod dystrophy was diagnosed when the patient exhibited a progressive decline in visual acuity, a central scotoma, and reduced cone and rod responses on full-field ERG, with cone function equally or more severely reduced than rod function. Atrophic changes to the macular were confirmed in each patient using ophthalmoscopy and OCT images. When the two graders disagreed with regard to the diagnosis, another retinal specialist (KO) arbitrated. We excluded patients with Stargardt disease, central areolar choroidal dystrophy, pattern dystrophy, vitelliform macular dystrophy, age-related macular degeneration, rod-cone dystrophy, cystoid macular edema, syndromic disorders, and systemic disease such as a malignant tumor or hematological malignancy. Patients with a media opacity that impaired image quality were also excluded. The right eye of each patient was chosen for analysis.

Clinical Assessment

We determined each patient's inheritance trait based on his or her family history. Best-corrected visual acuity was obtained from each patient using Landolt C charts. These values were then converted to the logMAR equivalent. All patients underwent dilated slit-lamp biomicroscopy, fundus examinations, and OCT imaging, which was performed using a spectral domain-OCT device (Spectralis; Heidelberg Engineering, Germany). As stated above, full-field ERG recording was performed according to the recommendations of the ISCEV 2008.[26] The protocol includes the following settings: dark-adapted 0.01 ERG (rod response); dark-adapted 3.0 ERG (combined rod-cone response); light-adapted 3.0 ERG (cone response); light-adapted 3.0 flicker (30-Hz flicker). The amplitude of each component was used for subsequent analyses.

Visual Field

Visual field testing was performed using a Goldmann perimeter (Haag Streit, Bern, Germany). The results were scanned and analyzed with ImageJ software (http://imagej.nih.gov/ij/; provided in the public domain by the National Institutes of Health, Bethesda, MD, USA). The magnification scale was calibrated first using the radius of the central 90° as is presented on standard recording paper. Under this system of calibration, a length of 632 pixels was equivalent to 10.8 cm on the visual field recording paper. The scotoma area, as defined by the I/4e white test light, was traced and measured with the software. We included the blind spot of Mariotte when it was included within the extended scotomal area. The results were given in square centimeter units.

Wide-Field Fundus Autofluorescence

Wide-field fundus photographs and FAF images were obtained with a ultra-widefield retinal imaging system. This instrument uses green light at 532 nm for excitation and captures the emitted signal with a detector for light from 570–780 nm. Although the retinal imaging system (Optos PLC) can acquire images from a nonmydriatic eye, we routinely dilated the pupils for concurrent OCT scans and ophthalmoscopic examinations.

We measured the area of abnormal FAF with ImageJ software (http://imagej.nih.gov/ij/; provided in the public domain by the National Institutes of Health, Bethesda, MD, USA). Any area of hypoautofluorescence or hyperautofluorescence was considered as abnormal FAF. To reduce the influence of eyelashes or eyelid shadow, we first excluded the most peripheral part of the image and cropped an elliptical area of 3000 × 2100 pixels from the original 3900 × 3072-pixel image for analysis (Fig. 1). Two of the authors (MO, AO), who were blinded to the patients' clinical characteristics, measured each image individually; the